Applied Water Science (2021) 11:48
https://doi.org/10.1007/s13201-021-01370-z

REVIEW ARTICLE

A critical review of synthesis parameters affecting the properties of zinc oxide nanoparticle and its application in wastewater treatment

E. Y. Shaba[1] · J. O. Jacob[1] · J. O. Tijani[1] · M. A. T. Suleiman[1]

Received: 5 October 2020 / Accepted: 18 January 2021

Abstract

In this era, nanotechnology is gaining enormous popularity due to its ability to reduce metals, metalloids and metal oxides into their nanosize, which essentially alter their physical, chemical, and optical properties. Zinc oxide nanoparticle is one of the most important semiconductor metal oxides with diverse applications in the field of material science. However, several factors, such as pH of the reaction mixture, calcination temperature, reaction time, stirring speed, nature of capping agents, and concentration of metal precursors, greatly affect the properties of the zinc oxide nanoparticles and their applications. This review focuses on the influence of the synthesis parameters on the morphology, mineralogical phase, textural properties, microstructures, and size of the zinc oxide nanoparticles. In addition, the review also examined the application of zinc oxides as nanoadsorbent for the removal of heavy metals from wastewater.

Keywords Zinc oxide · Synthesis parameters · Nanoadsorbent · Heavy metals

Introduction

Zinc oxide nanoparticles constitute one of the important metal oxides materials that have been widely applied in materials science due to its unique physical, chemical, and biological properties such as biocompatible, environmentally friendly, low cost and non-toxic nature (Alwan et al. 2015; Salahuddin et al. 2015; Ruszkiewicz et al. 2017). Owing to its exceptional properties, ZnO nanoparticles have been applied as a functional advanced material to solve different societal problems especially in the field of catalysis for wastewater treatment and also as cosmetics and antimicrobial additives (Ruszkiewicz et al. 2017). ZnO nanoparticles have several advantages which include unique chemical and thermal stability, robustness, and long shelf life over other metal oxides such as TiO_2, WO_3, SiO_2, and Fe_2O_3. Zinc oxide exists in the following phases: hexagonal quartzite, cubic zinc blende, and cubic rock salt (Belver et al. 2019). The wurtzite structure is the most common due to its stability at ambient conditions, where every zinc atom is tetrahedrally coordinated with four oxygen atoms (Barhoum et al. 2019). In each phase, zinc oxide nanoparticles (ZnONPs) are a semiconductor material with a direct wide bandgap of ~ 3.3 eV (Senol et al. 2020). It has advantages such as stabilization on substrate especially the zincblende form with a cubic lattice structure (Parihar et al. 2018). Food and Drug Administration (FDA) includes also zinc oxide as one of the safest metal oxides that can be used in food industries (Bettini et al. 2016).

Zinc oxide nanoparticles have been synthesized via different chemical and physical methods, namely sol–gel, hydrothermal, precipitation and co-precipitation, chemical vapour deposition, spray pyrolysis, magnetic sputtering, microwave-assisted technique, solvothermal, biological routes amongst others (Ul-Haq et al. 2017). Each of the listed methods has advantages and disadvantages and as such different morphologies of ZnO nanoparticles according to characterization tools ranging from nanoplates, nanostars, nanobelts, nanotubes have been reported (Ambika and Sundararajan 2015). Different zinc salts such as zinc acetate dehydrate ($ZN(C_2H_3O_2)_2{\cdot}2H_2O$)), zinc nitrate hexahydrate ($Zn(NO_3)_2{\cdot}6H_2O$) zinc sulfate ($Zn(SO_4)_2{\cdot}7H_2O$) and zinc chloride ($ZnCl_2$) as precursor have been used to prepare ZnO nanoparticles (Ambika and Sundararajan 2015; Ezhilarasi et al. 2016; Sierra et al. 2018).

However, the problems of stability, dispersion and crystalline structures control of ZnO nanoparticles in aqueous

✉ E. Y. Shaba
elijah.shaba@futminna.edu.ng

[1] Department of Chemistry, Federal University of Technology, P. M. B. 65, Minna, Niger State, Nigeria

Published online: 13 February 2021

medium constitute a serious bottleneck to industrial application of the material. In order to surmount the challenges, many researchers have focused on the investigation of factors affecting the properties of stable zinc oxides- nanoparticles (Yu and Dong 2016). These factors include pH of the reaction mixture, synthesis and calcination temperature, reaction time, concentrations of precursors, solvent medium and surfactant concentration among others (Hajiashafi and Motakef-Kazemi 2018). The aforementioned factors directly influence the particle size, morphology, phase, and surface area of the zinc oxide nanoparticles (Hajiashafi and Motakef-Kazemi 2018; Perillo et al. 2018; Jamal et al. 2019).

Zinc oxide nanoparticles display some properties such as high chemical and thermal stability, unsaturated surfaces, and excellent adsorption behaviour towards organic and inorganic pollutants in aqueous matrix. ZnO nanoparticles possess higher photon absorption efficiency, high surface area, and oxidizing power compared to the other semiconductors and are easily available, non-toxic, and cost-effective for the purification of wastewater (Ray and Shipley 2015). These characteristics have encouraged many scientists in recent years to study the adsorptive potentials of ZnO nanoparticles for the removal of heavy metals from industrial wastewater (Yuvaraja et al. 2018). Different shapes of ZnO nanoparticles have been reported to have high removal efficiency for heavy metals. For instance, a spherical shape ZnO nanoparticles removed lead (Pb^{2+}), cadmium (Cd^{2+}) and mercury (Hg^{2+}) from aqueous solution (Angelin et al. 2015). Additionally, ZnO nanorods, flowers and nanocubes were used as nanoadsorbent to remove arsenic (As^{3+}), chromium (Cr^{6+}) from wastewater (Yuvaraja et al. 2018). Several researchers have synthesized ZnO nanoparticles based on the variation of different process parameters such as pH, stirring speed, reaction time, reaction temperature, mixing ratio, calcination temperature and precursor concentration. However, there is a paucity of information on the comprehensive review on the effects of these synthesis parameters on the shape, size, and phase of zinc oxides. Not only that, the application of ZnO nanoparticles as nanoadsorbent has also not been comprehensively reported by researchers. Herein, the review of some of these process parameters such as the effect of pH, reaction time, and synthesis and calcination temperature on the properties of zinc oxide nanoparticles such as morphology, crystallite size, and surface area is provided. The review also focuses on the application of ZnO nanoparticles as nanoadsorbent for the removal of heavy metals in different wastewater.

Crystal structure of zinc oxide nanoparticles

Zinc oxide (ZnO) is a water insoluble white powder used as an additive in different products especially foods, paints, sunscreens, lubricants, sealants, and batteries (Chandramohan et al. 2017; Perveena et al. 2020). Although ZnO occurs naturally as the mineral zincite, most zinc oxides are chemically produced under different conditions in the laboratory. Zinc oxide nanoparticles can exist in three forms, namely hexagonal-wurtzite, cubic zincblende, and cubic rocksalt (see Fig. 1). The shaded black and gray spheres represent oxygen and zinc atoms (Wang and Zhang 2005). The wurtzite structure is most common and stable at ambient conditions due to its ionicity that resides exactly at the borderline between the covalent and the ionic materials (Chandramohan et al. 2017). The zinc blend ZnO structure can only be stabilized by growing on cubic substrates and the rocksalt structure can be obtained at relatively high pressures, 10 GPa (Özgür et al. 2005). As found with most group II-VI elements, the bonding in ZnO is largely ionic with 0.074 nm for zinc ions (Zn^{2+}) and 0.140 nm for the oxygen ion (O^{2-}) as corresponding radii. This property is responsible for the preferential formation of wurtzite rather than zinc blend structure (Phillips), as well as its high piezoelectricity.

Classification of zinc oxide nanomaterials

Classification of ZnO nanoparticles is based on the number of dimensions, which are not confined to the nanoscale range (< 100 nm). The main types based on the dimensions and structures are: zero-dimensional (0D), one-dimensional (1D), two-dimensional (2D), and three-dimensional (3D) nanomaterials (Zhang et al. 2018) and their detail descriptions and morphological properties are provided in Table 1.

Morphology of ZnONPs

Different morphologies of zinc oxide nanoparticles have been reported by researchers due to the variation of various process parameters. These include nanorods (Ghannam et al. 2019), nanowires (Hu et al. 2007), nanospheres (Nejati et al. 2016), nanoflowers (Peng et al. 2013), nanotubes (Wang and Cui 2009), nanotetrapods (Jin et al. 2013), nanoplate (Tan et al. 2015) and nanotripods (Azhar et al. 2017). The formation of different morphologies of ZnO nanoparticles shown in Table 2 depends on the applied synthesis conditions.

Table 2 shows a description of different morphologies of ZnO nanoparticles synthesized by different researchers. The table revealed different morphologies of ZnO nanoparticle such as nanospheres, nanorods, nanoflowers,

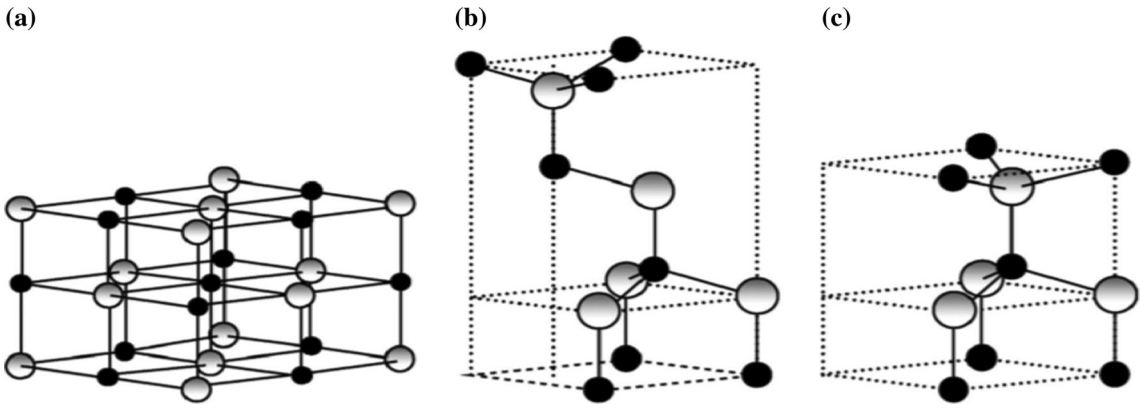

Fig. 1 Different phases/network structures of ZnO nanoparticles **a** cubic rocksalt, **b** cubic zincblende, **c** Hexagonal-Wurtzite

Table 1 Different dimension and descriptions of zinc oxide nanoparticles

Dimensional	Description	Nanomaterial type	Morphology	References
Zero dimensional (0D)	All the dimensions (Length, breadth, and heights) are in existence in the nanoscale (< 100 nm), 0D nanostructures are the simplest building blocks that can be used to design and create 1D, 2D, and complex 3D nanostructures	Nanoparticles and nanodots		Cao (2017)
One dimensional (1D)	Two dimensions are in the nanoscale (1–100 nm) and the other one dimensions in macroscale	Two dimensions nanomaterials have needles like-shaped such as nanowires, nanofibers, nanorods, nanocapsule, nanowalls and nanotubes		Nasrollahzadeh et al. (2019)
Two dimensional (2D)	In two-dimensional nanomaterial (2D), the two dimensions are outside the nanoscale	They exhibit plate-like shapes such as nanofilms, nanoplates nanolayers, and nanocoatings	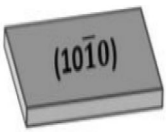	Leonardi (2017)
Three dimensional (3D)	The three dimensions are not in nanoscale and all dimensions are in macroscale	Nanocomposites	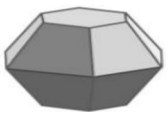	Tseng et al. (2012)

nanotubes, nanotetrapods, nanoplates and nanotripods obtained under different synthesis conditions and synthesis methods in the laboratory. The formation of the desired shape of ZnO nanoparticles depends on the role played synthesis parameters such as solution pH, template agents, reaction temperature, reaction time, stirring speed, solvent types, calcination temperature, calcination time and others. The effects of some of the aforementioned factors on the properties of ZnONPs irrespective of the synthesis approach are explained as follows:

Factors influencing the synthesis of ZnO nanoparticles

pH of reaction mixture

pH of the reaction mixture determines the types of ZnO nanoparticles formed (Aziz and Jassim 2018). The crystallite size, morphology, phases, and surface areas of ZnO nanoparticles depend largely on the amount of positively and negatively charge ions present in the medium dur-

Table 2 Different morphology of zinc oxides methods and reaction conditions of ZnO nanoparticles

Nanomaterial	Method of Synthesis	Description	Morphology	References
Nanotubes	Chemical Precipitation	A nanotube is a tube-like structure that belong to one-dimensional (1D) nanostructure group (Erhard and Holleitner 2015)	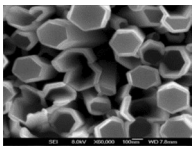	Wang and Cui (2009)
Nanotetrapod	Chemical vapour transport	Nanotetrapods are nanomaterial with four feet that belong to the dimensional structure. The advantage of nanotetrapods over other nanocrystalline geometric shapes of nanomaterials includes alignment with themselves spontaneously to the plane with one standard 'arm' (Marcus et al. 2007). ZnO nanotetrapod legs are spatially distributed with an angle of 109.5° (Modi 2015)	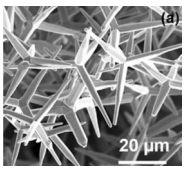	Jin et al. (2013)
Nanosphere	Precipitation	The nanosphere is the simplest form of nanoparticle with only one adjustable geometric parameter (radius) exhibiting resonant responses under optical excitation (Ahmadivand et al. 2016)	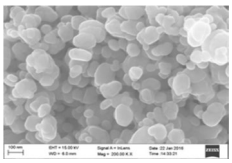	Geetha et al. (2016)
Nanowires	Hydrothermal	Nanowire is a solid rod-like structure having thickness or diameter constrained to tens of nanometers or less (1 nm = 10^{-9} m) that is similar to conventional wires (Waqar et al. 2015). Nanowires are known as 1D material due to the large difference between their diameter and length (Nasrollahzadeh et al. 2019). Nanowires have been reported to have fewer structural defects over their bulk counterpart (Erhard and Holleitner 2015)	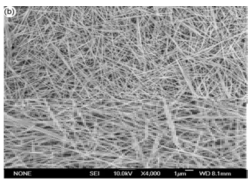	Hu et al. (2007)
Nanoflowers	Hydrothermal	Nanoflowers are nanostructure similar to plant flowers in a nanoscale range that is usually prepared in extreme conditions like 80–550˚C (Shende et al. 2018). Nanoflowers have also been reported to have a high volume-to-surface ratio which improve surface adsorption that can speed up reaction kinetics (Goryacheva 2016)	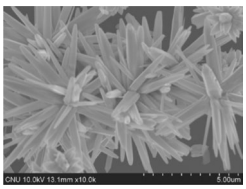	Eadi et al. (2017)
Nanoplates	Hydrothermal	Nanoplate is a nanomaterial that has plate-like structure or have two-dimensional nanostructures (2D) (Peng et al. 2017)	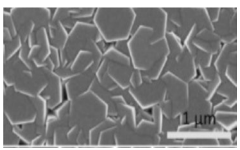	Tan et al. (2015)

Table 2 (continued)

Nanomaterial	Method of Synthesis	Description	Morphology	References
Nanorods	Sol–gel	Nanorods are nanostructures that have rod-like shape. Nanorods have one dimension outside the nanoscale. Nanorods have unique advantage over other one dimension nanostructure due to the fact that it can be made from most elements (metals and nonmetals) and compounds, and simple synthetic methods compared to nanotubes and nanowires (Ghassan et al. 2019)	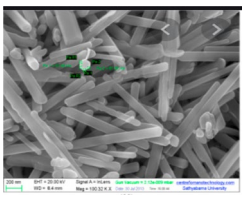	Meenakshi and Sivasamy (2017)
Nanotripods	Hydrothermal	A nanotripod is a nanomaterial that is like a portable tee-legged frame or stand with a two-dimensional nanostructure with planar arms that appear as rectangular nanoplates (Al-Sarraf et al. 2018). Zinc tripod is a two-dimensional (2D) nanostructure	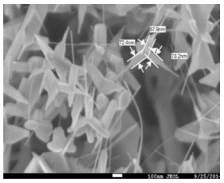	Azhar et al. (2017)

ing the preparation (Chitha et al. 2015; Swaroop and Somashekarappa 2014). This is because solution pH alters the electrical charge of molecules and such alteration will affect their reduction (Hasan et al. 2018). During the synthesis of ZnO in an acidic medium (pH < 7), the amount of hydroxyl ions (OH^-) is usually low in the solution which hinders hydrolysis and condensation processes, leading to the smaller aggregates at the end of poly-condensation process (Tourné-Péteilh et al. 2018). The decrease in the crystallite size of the zinc nanoparticle in an acidic medium was attributed to the preferential corrosion of the ZnO crystal structure (Rafaie et al. 2014). At the pH of 7 (neutral), the hydrogen ion (H^+) and the hydroxyl ion (OH^-) concentrations are equal, therefore, making the solution having little or no influence at the interfaces of zinc oxide crystals (Mohammadi and Ghasemi 2018). When the pH of the reaction mixture is greater than 7, the number of OH^- ions is usually high causing strong attraction between the positively charged Zn^+ and OH ion; subsequently, increase crystallization and formation of a smaller ZnO nanoparticle. Under high concentration of the hydroxyl ions in a solution, intermediate products such as zinc hydroxide ($Zn(OH)_2$) (see Eq. 1) and salt-containing tetrahydroxozincate ion ($[Zn(OH)_4]^{2-}$) (see Eq. 2) are formed (Rafaie et al. 2014). The drying in the oven and calcination of the products in the furnace as shown in Eqs. (1) and (2) usually lead to the formation of zinc oxide nanoparticles of large crystallite size (Buazar et al. 2016).

The reaction mechanism of growth of ZnO nanoparticles with respect to variation of solution pH from acidic to basic region is shown in Eqs. 1–6

$$Zn^{2+} + 2OH^- \leftrightarrow Zn(OH)_2 \quad (1)$$

$$Zn(OH)_2 + 2OH^- \leftrightarrow [Zn(OH)_4]^{2-} \quad (2)$$

$$[Zn(OH)_4]^{2-} \leftrightarrow ZnO_2^{2-} + 2H_2O \quad (3)$$

$$ZnO_2^{2-} + 2H_2O \leftrightarrow ZnO + 2OH^- \quad (4)$$

$$ZnO + OH^- \leftrightarrow ZnOOH^- \quad (5)$$

$$ZnOH^- + Na^+ \leftrightarrow ZnOOH - Na \quad (6)$$

The $[Zn(OH)_4]^{2-}$ formed in Eq. (2) can also exist in the form of $Zn(OH)^+$, $Zn(OH)_2$, or $Zn(OH)^{3-}$, depending on the process parameters, such as the concentration of the zinc ion (Zn^{2+}) and hydroxyl ion (OH^-) ion during the chemical reaction (Purwaningsih et al. 2016). When the concentration of Zn^{2+} and OH^- reaches the super-saturation degree, ZnO nuclei are formed based on reaction (4) (Osman and Mustafa 2015). The previous findings showed that the pH of the reaction mixture influenced the crystallite size and the morphology of zinc oxide nanoparticles. Researchers such as Ogbomida et al. (2018) reported the synthesis of ZnO nanoparticles via sol–gel method using Zn $(CH_3COO)_2{\cdot}2H_2O$ and NaOH as starting materials. The mixture was stirred for 2 h and subsequently dried for 1 h. ZnO nanoparticles produced were characterized using XRD, SEM, and UV–visible/diffuse reflectance spectroscopy and the calculated crystallite sizes 49.98 nm, 48.31 nm, 38.32 nm, and 36.65 nm for the

solution pH of 8, 9, 10 and 11, respectively. The authors found that the ZnO nanoparticles formed were mostly spherical in shape with an optimum solution pH of 9. On the contrary, Ikono et al. (2012) employed Zn $(CH_3COOH)_2{\cdot}0.2H_2O$ as a precursor, NaOH (precipitating agent) and ethanol solutions to prepare ZnO nanoparticles via sol–gel. The mixture was stirred for 2 h at 25 °C after which the precipitates were washed and dried for 15 min at 80 °C and the size of the crystals formed was directly proportional to the solution pH. The crystallite size increases from 10.94, 17.44, and 38.27 to 74.04 nm with a corresponding increase in the solution pH from 7, 8, 10, and 12, respectively. More so, the mineralogical phase of the prepared ZnO nanoparticles was examined using XRD and the authors observed that as the solution pH increases from 7, 8, 10, and 12, the purity of ZnO nanoparticles also increases and the percentage yield increased from 42.9%, 62.2%, 64.7%, to 100%, respectively. The differences in the crystallite size were linked to the reaction conditions used during the synthesis of the ZnO nanoparticle. In addition, Goryacheva (2016) demonstrated the green synthesis of ZnO nanoparticles using an aqueous extract of *Citrus aurantifolia* as a stabilizer and zinc nitrate as zinc salt precursor. The synthesis was carried out at 90 °C at pH 5, 7, and 9, respectively. The precipitates formed were washed, dried and annealed in air at 300 °C yielding nanorods with a crystallite size of 100 nm. XRD and SEM analysis confirmed the formation of pure hexagonal wurtzite ZnO nanostructure of different shapes irrespective of solution pH. The authors reported spherical shape at pH 5 and nanorods at pH of 7and 9, respectively. The increase in particle size and change in the morphology of the ZnO nanoparticles synthesized at the pH of 5, 7, and 9 further suggest that solution pH plays an important role in the crystallite size and morphology of ZnO. The results and other research findings carried out by different workers on the effect of solution pH on the crystallite size and morphology on the synthesis of ZnO nanoparticles are summarized in Table 3 as follows.

Table 3 shows the result of analysis from different researchers due to variation of solution pH. The results revealed that the solution pH plays an important role during the synthesis of ZnO nanoparticle. The ZnO nanoparticles synthesized at lower solution pH (acidic medium) had a smaller crystallite size irrespective of the method and the reaction conditions compared to the neutral and basic medium. This is an indication that the acidic medium affects the ZnO crystal structure leading to the formation of smaller crystallite sizes. At a higher solution pH, a different trend was observed by different authors as shown in Table 3 due to the formation of an intermediate compound, which allows the formation of larger crystallite size. Generally different morphologies of ZnO nanoparticles were observed at different solution pH and the crystallite size is a function of solution pH.

Reaction temperature

The physical methods mostly employed to synthesize nanoparticles require a higher temperature above 350°C, while chemical route used for the synthesis of nanoparticles can be carried out at room temperature (Kvitek et al. 2016). The chemical method is the easiest way to synthesize ZnO nanoparticles (Ul-Haq et al. 2017). It has been reported that higher temperature resulted to increase in reaction rate causing rapid consumption of metal ion and hence formation of nanoparticle of a smaller size (Kumari et al. 2016; Saxena et al. 2016). On the contrary, another researcher reported a smaller size of ZnO nanoparticle even at a lower temperature (Pelicano et al. 2016). However, a study by Liu et al. (2020) observed that reaction temperature played critical role in the actual crystallite size of nanoparticles so also the concentration of metal salt precursors. The authors found that low concentration of the precursors often leads to the formation of smaller crystalline size either at a lower or higher temperature, due to the competition between nucleation and growth processes. The research by Pushpanathan et al. (2012a) showed a reduction of particle size from 26 to 17 nm when the temperature of the reaction medium was increased from ambient temperature to 50 °C. The synthesized ZnO nanoparticles were characterized by SEM, XRD, and UV–visible spectrophotometer. From their result, it was noticed that an increase in reaction temperature resulted to a quick reduction of Zn^+ ions and subsequent formation of ZnO nanoparticles with a smaller crystallite size. It was also suggested that synthesis of ZnO nanoparticles carried out at lower temperature can also lead to formation of smaller crystallite sizes while at higher temperature nucleation was more favoured. Research by Khan et al. (2014) revealed that employing zinc acetate dihydrate, NaOH and cetyltrimethylammonium bromide (CTAB) as precursors produced flower-shaped like ZnO nanoparticle at different reaction temperatures (25 °C, 35 °C, 55 °C, and 75 °C). The synthesized ZnO nanoparticles were examined using XRD, SEM, EDS, and UV–visible spectrophotometer. The authors revealed average crystallite sizes to be 23.7 nm, 82.5 nm, 69.6 nm, and 88.8 nm for ZnO nanoparticles prepared at 25 °C, 35 °C, 55 °C, and 75 °C, respectively. The increase in the crystallite size of the ZnO nanoparticle in a solution as the temperature increases was attributed to two phenomena, namely Oswald ripening and oriented attachment as shown in Fig. 2. The SEM results showed the existence of two types of flower petal morphologies (slender needle-like and wide-arrow-like). The slender needle-like petals were found in excess at lower temperatures compared to the large arrow-like petals in the different flower bunches of the ZnO colonies. These observations suggested that the temperature exerted great influence on the crystallite size and morphology of the ZnO nanoparticles. The differences as reported by the previous

Table 3 Effect of variation of solution pH on the properties of ZnONPs

Methods	Precursor zinc salt	Other reagents	pH	Other synthesis conditions	Characterization techniques	Crystallite size (nm)	Research findings	References
Sol–gel	Zinc acetate dihydrate	NaOH	6, 8, 12 and 13	Stirred at 30 ºC for 7 h	XRD, SEM, PL, UV–Vis	13.8, 18.0, 24.7 and 33	The authors found that the morphology of the ZnO nanoparticles changes from roughly spherical to rod-like structure as the pH of the solution increases. These changes in morphology indicated that the increase in pH has a greater impact on the morphology of the ZnO nanoparticles	Chitha et al. (2015)
Precipitation	Zinc nitrate hexahydrate	Ammonia and ethanol	7.5, 8.0 and 8.5	Stirred at room temperature followed by calcination at 250 ºC for 2 h	SEM and XRD	23.21, 21.43 and 17.41	Mixture of nanocapsules and nanospherical like were obtained at solution pH of 7.5 and 8.0 while an irregular shapes ZnO nanoparticles were observed for pH 8.5	Dange et al. (2015)
Co-precipitation	Zinc nitrate hexahydrate	Sodium hydroxide	7, 9, 10.5, 12.5	Stirred at room temperature and dried at 110 ºC for 6 h	XRD, SEM, FTIR and UV–vis	31, 28, 21 and 16	They also established that ZnO nanorods were formed at solution pH of 7 and 9, while plate-like structures were observed at pH values 10.5 and 12.5, respectively. The pH of the reaction medium did not only affect the crystallite size but also influence the obtained morphology	Shende et al. (2018)
Green route	Zinc acetate dihydrate	*Citrus aurantifolia* juice	5, 7 and 9	Stirred at 90° C for 2 h, left for 24 h at room temperature and calcined at 300 °C for 6 h	SEM, EDX, XRD and PL	100	ZnO nanorods were formed at irrespective of solution pH	Rafaie et al. (2014)

Table 3 (continued)

Methods	Precursor zinc salt	Other reagents	pH	Other synthesis conditions	Characterization techniques	Crystallite size (nm)	Research findings	References
Precipitation	Zinc nitrate hexahydrate	Ammonia	8 and 12	Stirred at 80 ° C for 5 min	XRD, SEM and UV–Visible spectroscopy	43 and 50	The estimated crystallite sizes were directly proportional to the solution pH and were attributed to the dissolution of zinc hydroxide irrespective of the medium. At solution pH of 8, the morphology consists of mixtures of flakes-like and flower-like structures. However, by further increasing the pH to 12, morphology of flower-like structures surrounded by few spherical nanoparticles	Koao et al. (2015)
Co-precipitation	Zinc acetate dihydrated	HCl, and NH_4OH	8, 9, 9.5 and 10	Stirred at 85 °C for 6 h and dried at 100 °C for 5 h	XRD, SEM,EDS and FTIR	131.8, 19.8, 17.9 and 52.7	The morphology changes from spherical and flower-like as the pH increases from pH 9.5 and 10, respectively, with the optima pH at 9.5	Purwaningsih et al. (2016)
Sol–gel	Zinc acetate dihydrate	ammonia and CH_3OH	9 and 11	Stirred at 100–150 ℃ for 2 h and dried at 100 ℃ for 1 h	XRD, SEM, AFM	12 and 30	It was found that the size of the nanoparticles increased from 12 to 30 nm with increase in pH from 9 to 11	Abdullah et al. (2017)

Table 3 (continued)

Methods	Precursor zinc salt	Other reagents	pH	Other synthesis conditions	Characterization techniques	Crystallite size (nm)	Research findings	References
Sol–gel	Zinc acetate dihydrate	NaOH	8, 9, 10, 11 and 12	Stirred for 8 h, dried at room temperature for 2 h calcinated at 100 C for 2 h	XRD, FTIR SEM and UV–Vis	28, 25, 29, 35 and 37	Excellent hexagonal crystalline ZnO nanorods were obtained at solution pH of 10 and 11, respectively. They found that ZnO nanoparticles can be obtained from the optimized pH value of the reaction mixture at 11 using Sol–gel synthesis	Ravangave and Shaikh (2017)
So-gel	Zinc acetate dihydrate	NaOH, CH_3OH	pH 8, 9, 10, 11 and 12	Dried temperature of 80 °C for 1 h	XRD	10.94, 17.44, 38.27 and 74.04	The authors established a direct proportionality between pH (7, pH 8, pH 10) and the purity of the ZnO nanoparticles (42.9%, 62.2%, 64.7%, and 100%)	Siswanto and Akwalia (2017)
Green route	Zinc acetate dihydrate	*Sarcopoterium spinosum, ethylene glycol*, HCl, NaOH	4, 7 and 10	Stirred at 60 °C for 2 h	SEM, EDX, XRD, UV–Vis	78.21, 63.47 and 31.81	A spherical, rod and plate-like shapes were obtained for ZnO nanoparticles prepared at solution pH 4, 7 and 10	Kahaman et al. (2018)
Sol–gel	Zinc acetate dihydrate	NaOH	7–11	Synthesized at room temperature	XRD, FTIR, FESEM, UV–vis and PL	59.56, 46.45	Spherical ZnO nanoparticles were obtained. The authors reported decrease in the crystallite size as the pH values increase. The authors found that the optimum pH to be 11	Ribut et al. (2018)

Table 3 (continued)

Methods	Precursor zinc salt	Other reagents	pH	Other synthesis conditions	Characterization techniques	Crystallite size (nm)	Research findings	References
Co-precipitation	Zinc chloride	NaOH	10, 11, 12, and 13	Stirred at 60 °C for 2 h, dried at 100 °C for 18 h followed by calcination at 550 °C for 5 h	XRD, SEM, FTIR and TEM. UV–Vis	100, 92.5, 61.8 and 41.9	The decrease in particle size as the pH increases was attributed to the fact that at higher pH values, super-saturation during co-precipitation was higher, promoting nucleation over growth, thus giving smaller particle sizes. The ZnO nanoparticles had no definite shape for all the pH, except at solution pH of 13 that exhibited a needle-shaped particle	Jamal et al. (2019)

workers (Pushpanathan et al. 2012a) may be due to the differences in synthesis methods and the nature of capping agents used. Similarly, Manzoor et al. (2015) reported the synthesis of ZnO nanoparticles via co-precipitation method using zinc acetate with potassium hydroxide and ethanol as precursors. The mixture was stirred for 1.3 h under the influence of different synthesis temperature from 65 °C, 70 °C to 75 °C. The final product was dried in the oven at 60 °C for 8 h and characterized using SEM, XRD, FTIR, and UV–visible spectrophotometer. The average crystallite sizes of the ZnO nanoparticle obtained at three studied temperatures were 98 ± 43, 135 ± 77, and 458 ± 243 nm, respectively. The authors established a direct relationship between the reaction temperature and crystallite sizes. Furthermore, Pelicano et al. (2016) employed precipitation method involving mixing zinc acetate dihydrate as the precursor, with ethanol and dimethyl sulfoxide; tetramethyl, ammonium hydroxide as solvent and precipitating agents to produce ZnO nanoparticles. The prepared ZnO nanoparticles were investigated by TEM, UV–visible spectrophotometer, and PL. The TEM result indicated an increase in crystallite size (4.72 nm, 5.24 nm, 6.70 and 7.61 nm) as the reaction temperature increases (26 °C, 40 °C, 60 °C and 80 °C). The authors attributed the increment in the crystallite size to the increase in the critical particle radius and coalescence of the smaller particles to complement the growth into larger based on Ostwald ripening (for more soluble materials) and oriented fixing (for less soluble crystals) as shown in Fig. 2.

From Fig. 2, the first stage in the synthesis of ZnO nanoparticles is the nucleation of a solid ZnO crystal (E1); this is made possible via rapid precipitation reaction of a zinc salt by the precipitating agents such as sodium hydroxide, $(NH_4)_2CO_3$ and NH_4OH (Herrera-Rivera et al. 2017). The second stage involved the growth of nucleus by diffusion of ZnO molecules from solution onto the surface of the nucleated particle (E2), followed by collision and fusion (E3) of two particles via the oriented attachment (OA) and E4 depict the Ostwald ripening (OR) which involved inter-particle growth via exchange (dissolution and diffusion) of molecules between various particles (Zhang et al. 2010). Other reported researches on the effect of reaction temperature on the crystallite size and morphology of the ZnO nanoparticles are summarized in Table 4.

Synthetic temperature plays a very vital role as shown in Table 4. The Table revealed that the crystallite size of the ZnO nanoparticles increases as the synthesis temperature increases except for the result reported by Indramahalakshmi (2017) who employed the green method for the synthesis of ZnONPs. This implies that the increase or decrease in the crystallite sizes of ZnO nanoparticles also did not only depend on the reaction temperature but also on the method of synthesis.

Calcination temperature

Calcination involves heat-treating a material at a controlled temperature and in a controlled environment. During the calcination process, the particles fuse and enlarge its primary crystallite size (Ruys 2019). This process is called particle coarsening, a phenomenon in solid (or liquid) solutions often used for the growth of larger crystals from those of smaller size and lead to reduction in the number of smaller particles while larger particles continue to grow (see Fig. 3). The particle coarsening phenomenon occurs due to the fact that the smaller nanoparticles are less energetic and unstable compared to the well-packed nanoparticle with a large crystallite size. This process can also take place at room temperature and however can be accelerated during heating process. Different researchers have studied the effect of calcination temperature on properties of zinc oxide nanoparticle and these are reviewed as follows: (Parra and Haque 2014) synthesized ZnO nanoparticles via aqueous chemical route using zinc acetate dihydrate and sodium hydroxide (NaOH) as precursor material for 15 min at 60 °C. The ZnO nanoparticles synthesized were identified by XRD, SEM, EDX, AFM and UV–visible spectrophotometer. The authors reported that as the calcination temperature increases from 200 °C, 400 °C to 500 °C, the particle size also increases from 30, 41, and 44 nm, respectively. Besides, Ashaf et al. (2015) studied the effect of calcination temperature on properties of ZnO nanoparticles by sol–gel using zinc acetate as a precursor. The XRD results indicated the formation of pure phase hexagonal wurtzite ZnO; however the crystallite size decreases from (24–17 nm) as the calcination temperature increased to 300 °C. Further increase in calcination temperature to 500 °C resulted to increase in the crystallite size to 19 nm. Moreover, a similar trend was reported by Mallika et al. (2015) that employed sol–gel method to prepare zinc oxide nanoparticles using zinc nitric and polyvinyl alcohol (PVA) as a precursor and stabilizing agent, respectively. The authors varied the calcination temperature from (400 °C, 500 °C, and 600 °C to 700 °C) at holding time of 1 h. The synthesized ZnO nanoparticles were characterized using XRD, SEM, EDS, FTIR, and UV–visible Spectrophotometer and the average crystallite sizes were 7, 23, 35, and 35 nm. The authors found that as annealing temperatures increase, the grain growth also increases in sizes. A similar trend was observed when citric acid (CA) was used as reducing agent under the same calcination temperature and holding time. They reported an increase in the crystallite size from 13, 23, 30, and 40 nm. ZnO nanoparticles have been synthesized by sol–gel technique using zinc acetate dihydrate and diethanolamine as the precursor materials. The effects of calcination temperatures (300 °C, 500 °C, 650 °C, 700 °C, and 750 °C) were studied. The properties of the ZnO nanoparticles were examined by SEM, XRD, FTIR, and UV–visible Spectrophotometer. The XRD result according to Scherer equation indicated that the crystallite size increased with increasing calcination temperature (Kayani et al. 2015). Generally, it was found that as the calcination temperature increases, the crystallite sizes of the ZnO nanoparticles increase which can also affect its purity and morphology.

Furthermore, the growth of ZnO nanoparticle usually occurs via two mechanisms, namely oriented attachment (OA) and Ostwald repining (OR). Oriented attachment is a physical process that is important during crystallization process and involved direct self-organization of the primary nanoparticles and subsequent conversion by interface fusion to single crystals through sharing a common crystallographic

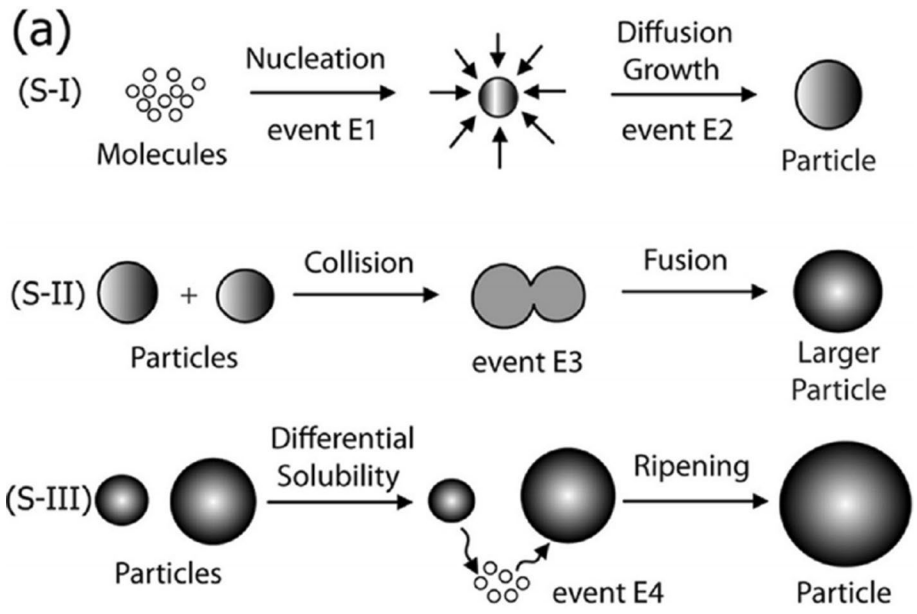

Fig. 2 Schematic of the stage wise-growth of ZnO nanocrystals in solution created based on the research by Layek et al. (2012)

Table 4 Effect of reaction temperature on the properties of ZnONPs

Methods	Precursor zinc salt	Other solvents	Temperature (°C)	Other Reaction conditions	Crystallite size (nm)	Characterization tools	Research findings	References
Co-Precipitation	Zinc acetate dihydrate	Methanol, potassium hydroxide	65, 70 to 75	Stirred 4° C for 10 min with speed 16 000 rpm dried in the oven at 60° C for 8 h and calcined 2 h	98 ± 43, 135 ± 77, 458 ± 243	SEM, XRD, FTIR and UV–Vis	XRD results suggested that faster growth dynamics at higher temperatures introduced defects and therefore reduced the quality of the crystals. The results clearly suggested increase in particle size with increase in reaction temperature	Manzoor et al. (2015)
Precipitation	Zinc acetate dihydrate	Ethanol and dimethyl sulfoxide	26, 40, 60 and 80	Centrifugation for 30 min	4.72, 5.24, 6.70, 7.61	TEM, UV–VIS and PL	The particles were hexagonal ZnO in shape with average sizes in the range of 4.72-7.61 nm as the reaction temperature increases	Pelicano et al. (2016)
Green route	Zinc acetate	*Opuntia ficus indica*	60 and 100	Stirred for 3 h	31.22, 24.44	SEM and UV–Vis, FTIR and EDX	The size of nanoparticle decreased with increase in temperature during the synthesis of ZnO nanoparticles	Indramahalakshmi (2017)
Green route	Zinc nitrate hexahydrate	Cherry fruit extract	25, 60 and 90	pH of 8, temperature stirred at 25 °C and for 12 h	87.5 to116	SEM, XRD, FTIR and UV–Vis	Spherical shape was obtained at synthesis temperature of 25 °C	Mohammadi and Ghasemi (2018)

Table 4 (continued)

Methods	Precursor zinc salt	Other solvents	Temperature (°C)	Other Reaction conditions	Crystallite size (nm)	Characterization tools	Research findings	References
Biosynthesis	Zinc nitrate hexahydrate	Pineapple peels	28 °C and 60 °C	Stirred at 60 °C for 48 h for 2 h	8–45	FTIR, FESEM, TEM EDX, and XRD	A mixture of spherical- and rod-shaped structures resulted from the synthesis of ZnO nanoparticles at 60 °C, while the synthesis carried out at 28 °C resulted in spherical flower-shaped structures. It was found that the crystallite size of ZnO nanoparticles prepared synthesis at 60 °C was small	Basri et al. (2020)
Biosynthesis	Zinc nitrate hexahydrate	Modified malt extract, glucose, yeast extract, peptone	20 °C and 40 °C	20 °C and 40 °C	8.2	TEM, SEM, AFM, EDS	The authors found that 14 fungal isolates were identified, having potential to reduce metal salt into metal nanoparticles	Raliya and Tarafdar (2013)
Chemical method	Zinc acetate dehydrate	Methoxyethanol, Monoethanolamine and NaOH	30 °C, 60 °C and 90 °C	Stirred at 60 °C for 24 h	45.5, 34.2, 39.3	SEM, XRD	The authors found that the morphology changed from spherical (30 °C) to a rod (60 °C) and ellipsoidal (90 °C)	Samei et al. (2008)
Green routes	Zinc acetate dehydrate	*H. sabdariffa* leaves	60 to 100	Stirred at 60 °C for 30 min, dried at 60 °C for 4 h	16–60	SEM, XRD, FTIR and UV–Vis	Sample prepared at 100 °C showed more crystallinity with a dumbbell-shaped structure compared with the sample at 60° C with less crystallinity and a spherical shape	Bala et al. (2015)

Table 4 (continued)

Methods	Precursor zinc salt	Other solvents	Temperature (°C)	Other Reaction conditions	Crystallite size (nm)	Characterization tools	Research findings	References
Precipitation	Zinc acetate dihydrate	NaOH	Room temperature to 50 °C	Stirred at 60 °C for 24 h	26 to 17	SEM, XRD, UV–Visible, FTIR	As the reaction temperature increased from room temperature to 50 °C, the particle size decreased from 26 to 17 nm	Pushpanathan et al. (2012b)

orientation (Cao et al. 2019), as illustrated in Fig. 3. Ostwald ripening involved diffusive transfer of the dispersed phase from the smaller to the larger droplets. The Ostwald Ripening occurs because larger particles are thermodynamically stronger than smaller particles. High temperature influences Ostwald ripening due to its effect on interfacial energy, coefficients of growth rate, and solubility (Westen and Groot 2018). Oriented attachment happens because the aggregation decreases the system's interphase boundary and total surface energy (Dalod et al. 2017). Previous works on the variation of calcination temperature on the properties of ZnO nanoparticles are summarized in Table 5.

Table 5 revealed direct relationship between calcination temperature and crystallite sizes. The higher the calcination temperature, the larger the crystallite size of the ZnO nanoparticles irrespective of the method, solvent and other synthesis conditions. Calcination temperatures also affect the morphology of ZnO nanoparticles and in most cases spherical shape of ZnO nanoparticles predominate.

Effect of different zinc salts precursor

The synthesis of ZnO nanoparticles using different zinc salts precursor such as zinc acetate ($Zn(CH_3COO)_2$, zinc nitrate($Zn(NO_3)_2$, zinc sulfate ($ZnSO_4$) and zinc chloride ($ZnCl_2$) has been widely investigated (Ambika and Sundararajan 2015; Ezhilarasi et al. 2016; Sierra et al. 2018). The use of different zinc salt precursors also influenced the morphological, textural and optical properties of ZnO nanoparticles (Mayekar et al. 2014). For instance, Gusatti et al. (2011) used different zinc salts ($ZnCl_2$ and $Zn(NO_3)_2{\cdot}6H_2O$) as precursors to synthesize ZnO nanoparticles. The mixture of zinc salts, ethanol and sodium hydroxide was stirred at 90 °C for 1 h and later the precipitate was washed severally and dried at 65 °C for a few hours. It was noticed that the average crystallites size of ZnO nanorods obtained using $ZnCl_2$ was 23 nm while morphology of ZnO nanoparticles prepared using $Zn(NO_3)_2{\cdot}6H_2O$ precursor was mixture of nanoprisms and nanorods shape with an average crystallite size of 18.91 nm. Also, Mayekar et al. (2014) utilized zinc nitrate, zinc chloride and zinc acetate and sodium hydroxide to prepare ZnO nanoparticles via sol–gel method. The mixture was maintained at 70 °C for 1 h, and the gel was later dried at 65 °C for several hours. The properties of the ZnO nanoparticle were identified using XRD, SEM, EDX, and UV–visible spectrophotometer, and it was found that the crystallite size was 36.06 nm (Nanoflowers), 38.90 nm (Rice-like), and 39.91 nm (Spherical) for ZnO nanoparticles prepared using zinc nitrate, chloride and acetate,

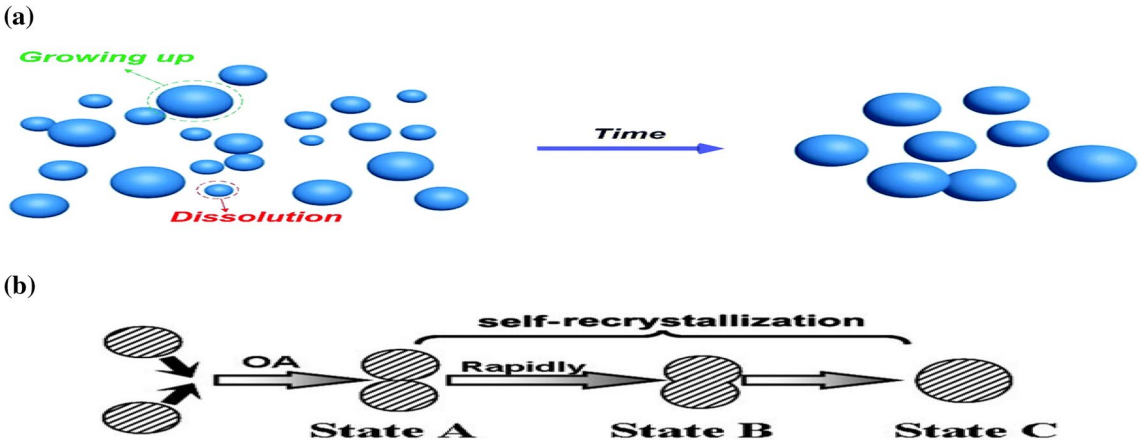

Fig. 3 Scheme of nanoparticle growth controlled by: **a** Ostwald ripening mechanism; **b** oriented attachment mechanism created based on the research by Kyoung-Ku et al. (2019)

respectively. The result also indicated that the ZnO nanoparticles synthesized using zinc acetate possessed highest purity while ZnO nanoparticles synthesized from using other zinc salts have similar crystallite size but different shapes. Moreover, Gusatti et al. (2011) employed hydrothermal method to synthesize ZnO nanoparticles using zinc nitrate, zinc acetate and zinc sulfate, sodium hydroxide as precipitating agent. The reaction was maintained at 120 °C for 3 h and dried at 70 °C. The ZnO nanoparticles produced were characterized by XRD, SEM, and TEM. The results showed successful synthesis of ZnO nanoflowers (100 nm), nanoflakes (125 nm) and nanoprisms (100 nm) from zinc nitrate, zinc acetate and zinc sulfate, respectively (Yu and Dong 2016). This implies that different zinc salts produced different shapes of ZnO nanoparticles with little or no effect on the crystallite size of zinc oxide nanoparticles. Different zinc precursors such as zinc nitrate ($ZnNO_3$), zinc chloride ($ZnCl_2$), and zinc sulfate ($ZnSO_4$) were used to synthesize ZnO nanoparticles via chemical precipitation method. The authors established that the crystallite size was the same (9.63 nm) irrespective of the zinc salt precursor and other synthesis conditions (Stirred at room at temperature for 2 h, dried at 80 °C for 15 h). This further confirmed that the source of precursor (Zn) from different zinc salts did not have any significant effect on the crystallite size of the ZnO nanoparticles produced. The influence of using different zinc salt precursors for the synthesis of ZnO nanoparticles as reported by different researchers is summarized in Table 6.

From Table 6, it is obvious that different zinc salts have little or no effects on the crystallite size of ZnO nanoparticles but greatly affect its morphology. Additionally, the variation in crystallite sizes of ZnO nanoparticles also depends on the adopted synthesis methods and other factors.

Concentration of precursors, precipitating and capping agents

The morphology and crystallite size of ZnO particles often depend on the concentration of metal salt precursors precipitating, and capping agents used (Phan and Nguyen 2017). Thus, these factors play an important role in the synthesis of ZnO nanoparticles and other nanostructured materials and thus very frequently used to avoid over growth of nanomaterial (Gulati et al. 2016). Capping agent is responsible for the control of growth rate, particle size, and prevention of particle aggregation (Bakshi 2015). Moreover, it has been reported by Al-Hada et al. (2014) that the nanoparticles can be stabilized by immobilization on a support such as organic ligand shell, polymers, dendrimers, cyclodextrins, and polysaccharides (See Fig. 4). The capping agents must be stable enough and withstand enough heat to prevent aggregation of the nanoparticles at temperatures suitable for synthesis (Gulati et al. 2016). Many researchers including (Borghei et al. 2013) have reported that the synthesis of ZnO nanoparticles using low concentration of zinc precursor always leads to the formation of nanoparticles of smaller crystallite size. In their research, zinc acetate dihydrate and sodium hydroxide, ethanol were mixed together and the particles formed were dried at 100 °C for 5 h and later calcined at 250 °C for 3 h to obtain ZnO nanoparticles with crystallite size ranging

Table 5 Influence of variation of calcination temperature on the properties of ZnONPs

Methods	Precursors	Other Solvent	Calcination Temperature (°C)	Other synthesis conditions	Crystallite size (nm)	Shape	Characterization techniques	Research Findings	References
Precipitation	Zinc nitrate hexahydrate	sodium carbonate (Na_2CO_3 and ethanol	250, 300, 350, 400, 500 and 600	Calcined for 2 h	14.58, 15.41, 28.33, 44.20, 72.50 to 91.44	Spherical	XRD, SEM, TEM, FT-IR and TGA	The result showed that the crystallite size increases with increasing annealing temperatures	Ruszkiewicz et al. (2017)
Sol–gel	Zinc acetate dehydrate	NaOH	100, 300, 500	Calcined for 2 h	24, 17,19.5	Spherical	XRD, SEM, UV–Visible spectrophotometer	The crystallite size decreases (from 24 to 17 nm) when calcination temperature increased to 300 °C. With further increase in calcination temperature, crystallite size increases to 19.5 nm	Parra and Haque (2014)
@Sol–gel	Zinc acetate dihydrate	Citric acid	400, 500, 600	Stirred at room temperature for 2 h dried at 60 °C for 4 h	31, 45, 53	Spherical	XRD, SEM, EDX, FTIR, UV–Visible spectrophotometer, PL	The crystallite sizes increase with increasing calcination temperature of the samples. The EDX analysis revealed only Zn and O as the dominant elements	Hedayati (2016)
Precipitation	Zinc nitrate hexahydrate	Ethylene glycol and hydrazine (N_2H_4)	400, 450, 500, 550, 600, 650	Air dry for 8 h	46–66	Spherical	XRD, TEM, FTIR, and UV–Visible spectrophotometer	The authors reported decreases in average particle size from 66 to 46 nm	Mornani et al. (2016)

Table 5 (continued)

Methods	Precursors	Other Solvent	Calcination Temperature (°C)	Other synthesis conditions	Crystallite size (nm)	Shape	Characterization techniques	Research Findings	References
Sol–gel	Zinc acetate dihydrate	NaOH	0, 100, 200, 300, 500, 700	Stirred for 2 h, dried in an oven at 100 °C overnight	32, 42, 62, 78, 92, 128	Spherical	SEM, XRD, UV Vis	The authors found that the average particle size of ZnO particles increases with increasing annealing temperatures	Shaikh et al. (2016)
@Co-precipitation	Zinc acetate dihydrate	NaOH	450, 600 and 750	Stirred at room temperature for 4 h, aged for 24 h at the same temperature, pH 10, Calcined for 2 h	31 nm, 33, 42,	Spherical	XRD, SEM and EDX	The XRD analysis revealed only hexagonal wurtzite ZnO phase without any impurities. Both degree of crystallinity and crystallite	
sizes increase with an increase in calcination temperature	Singh et al. 2016)								
Sol–gel	Zinc nitrate hexahydrate	Gelatin solution	450, 700 and 1000	Annealed for 3 h	70	Rod and spherical	XRD, TEM, and FTIR, PL, RS	ZnO nanoparticles with nanorods and platelets turn into quasi-spherical hexagonal wurtzite at a temperature of 1000 °C	Etcheverry et al. (2017)
Precipitation	Zn nitrate hexahydrate	Sucrose	400,500, 600, 700, 800	Stirred at room temperature and furnace at 400 °C	42.49, 52.72, 80.95 and 100.120	Spongy like material at 400 °C, a spherical shapes other temperatures	XRD, FESEM	Average size of synthesized ZnO nanoparticles increases with increasing annealing temperatures	Verma et al. (2017)

Table 5 (continued)

Methods	Precursors	Other Solvent	Calcination Temperature (°C)	Other synthesis conditions	Crystallite size (nm)	Shape	Characterization techniques	Research Findings	References
Precipitation	Zinc nitrate hexahydrate	PVA, NaOH	400, 500 and 600	Stirred at 70 °C for 12 calcined at 400 °C	22, 24 29	Spherical	XRD, SEM, FTIR, UV–Visible spectrophotometer	The XRD pattern and SEM images confirmed formation of hexagonal wurtzite phase of ZnO nanoparticles and the authors also found that crystallite size is directly proportional to the calcination temperature	Belay et al. (2018)
Co-precipitation	Zinc acetate dihydrate	Oxalic acid, Acetate and 2-propanol and oxalic acid	400, 500, and 600	Stirred at room temperature	3, 28, 25	Spherical	XRD, TEM, UV–Visible spectrophotometer	The authors found that as the calcination temperature increases (400°C, 500°C, and 600°C); a narrow size distribution of ZnO nanoparticles with average particle sizes of 3, 28, and 25 nm was observed, respectively	Baharudin et al. (2018)
Wet precipitation	Zinc nitrate hexahydrate	Ethylene glycol [CH_2(OH) CH_2OH]Citric acid	200, 400, 600 and 800	Stirred at 50–80° C for 3 h, dried at 150 ℃ for 4 h and pH 4	14, 22, 26 and 37	Semi-sphere and nearly hexagonal	XRD, SEM, TEM and PL	The average crystallite sizes increased progressively with annealing, and ranging between 13 and 39 nm	Aljawfi et al. (2020)

from 20, 27, 30 to 36 nm at different mixing ratio of sodium hydroxide to zinc salts precursor (1:1, 1:2, 1:3, and 1:4), respectively. Different morphologies such as Cauliflower-like, irregularly shaped, and non-uniform were obtained by increasing the concentration ratio of the reactant raw materials. From this result, it was suggested that a higher ratio of sodium hydroxide/zinc salt precursor resulted to the formation of larger crystallites size of ZnO. Similarly, Alami et al. (2015) employed spray pyrolysis method to prepare ZnO nanoparticles using different concentrations of Zn $(NO_3)_2$, $6H_2O$ (0.05, 0.1, and to 0.2 M). The reaction was carried out at solution spray rates of 2 ml/min onto a preheated glass substrate at 500 °C for 10 min. The crystallite sizes obtained were 9.95, 27.40, and 32.35 nm for 0.05, 0.1, and 0.2 M concentration of the Zn salt which confirm the earlier analysis that the concentration of zinc salt greatly affects the crystallite size of the ZnO nanoparticles.

Table 7 contains summarized works on the effects of salt precursor, precipitating and capping agents on the nature of ZnO nanoparticles carried out by different researchers.

Table 7 reveals that as the concentration of the zinc salt precursors increases, the crystallite size of ZnO nanoparticle produced also increased. Similarly, the crystallite sizes of the zinc oxide nanoparticles also increases as the concentration of the PVA and NaOH increases, respectively.

Reaction time

Reaction time is the time required for completion of all steps during the synthesis of nanoparticles including the reduction and formation of nanoparticles. Reports have shown that the formation of nanoparticles starts within minutes after the addition of the metal salt precursors and increases as the reaction time increases (Chitra and Annadurai 2014). For instance, Manzoor et al. (2015) prepared ZnO nanoparticles via co-precipitation method using zinc acetate with potassium hydroxide and ethanol as precursors. The final product was dried in the oven at 60°C for 8 h and characterized using SEM, XRD, FTIR, and UV–visible spectrophotometer. The mixture was stirred for 1.3 h by varying the nucleation time and they found that the crystallite size of the ZnO nanoparticles to be 20, 24, and 57 nm for nucleation time of 0, 2, 8 min. The authors found the ZnO nanoparticles have a nearly spherical shape with narrow particle size distribution. From the result above, it can be deduced that the reaction time is proportional to the crystallite size of ZnO nanoparticles. The step by step involved on the variation of reaction time during the synthesis of ZnO nanoparticles is shown in Fig. 5.

The first step 1(T_1) in Fig. 5 depicts the nucleation process (the process whereby nuclei (seeds) act as templates for crystal growth) which is the first step in the formation of ZnO oxide nanoparticles. This process takes place within a few seconds of the reaction (Thanh et al. 2014). Step 2 involves the growth of the nanoparticles up to an average crystallite size of 5.2 nm as the time increases from T_1 to T_3. However, it has been reported by Smolkova et al. (2017) that diffusion mechanism controlled the growth of nanoparticles during the synthesis which only occurs over a few seconds. The fourth stage is a rapid consumption of the zinc salt left in solution where the particle size increases rapidly from 5.2 to 7.7 nm. ZnO nanorods have been successfully synthesized by combination of sol–gel and chemical precipitation methods using zinc acetate and sodium hydroxide as starting materials. The authors reported crystallite particle size of 33 nm, 35, 38, and 42 nm for different synthetic time (2, 4, 6, and 8 h), respectively. The synthesized ZnO nanoparticles were dried in the oven at 100 °C for 2 h and later calcined at 100 °C for 2 h. The prepared ZnO nanoparticles were characterized by XRD, FTIR, SEM, UV–visible spectrophotometer and PL and it was established that the nucleation time affects the crystallite sizes of ZnO nanoparticles. Their result indicates that the crystallite size increases as the nucleation time increases. Similar trends have been reported by various researchers as summarized in Table 8.

Table 8 shows that different crystallites size is a function of nucleation time. A longer nucleation time leads to the formation of larger crystallite size. This trend observed in Table 8 may be because the particles have enough time to fuse and further fusion yielded large ZnO.

The effect of other synthesis conditions on the surface area, porosity and the crystal structure of ZnO

In evaluating the adsorption capacity of any adsorbent, surface area and the total pore volume play an important role. Studies have shown that the high surface area of ZnO nanoparticles, the greater adsorptive capacity and better the removal rate of heavy metal ions in wastewater (Shaikh and Ravangave 2015). The effects of other synthesis conditions or factors are on the textural properties, and crystals structure of ZnO nanoparticles is summarized in Table 9.

Table 6 ZnO nanoparticles synthesized based on variation of the different zinc salts precursor

Methods	Zinc salt	Other solvents	Synthesis conditions	Crystallite size (nm)	Characterization techniques	Shape	Research findings	References
Hydrothermal	Zinc nitrate hexahydrate, zinc acetate dihydrate, zinc sulfate heptahydrate	Potassium hydroxide	Autoclave at 120 °C for 3 h dried at 70 °C	100, 200, 50–200	XRD, SEM, TEM, PL	Nanoflowers, Nanoflakes, Nanoprisms	ZnO nanoparticles prepared from zinc nitrate possessed fewer oxygen vacancies and defects, while acetate and zinc sulfate sample with smaller particle sizes had more oxygen vacancies and defects	Yu and Dong (2016)
Precipitation	Zinc nitrate hexahydrate, zinc acetate dihydrate	NaOH, nitric acid and di-methyl sulphoxide (DMSO)	Stirred for 2 h at 70 °C, dried at 160 °C for 2 h, and calcined at 300 °C for 5 h	28.09, 31.86	XRD, SEM, FTIR, UV–Vis	Nanosphere, Nanorod	The differences in crystallite size and shape of ZnO nanoparticles using different precursors may be due to the different calcination temperature and holding time used Zn $(NO3)_2{\cdot}6H_2O$ (300 °C for 5 h) and $Zn(CH_3COO)_2{\cdot}2H_2O$ (400 °C for 12 h)	Getie et al. (2017)
Precipitation	Zinc nitrate hexahydrate, zinc nitrate hexahydrate, zinc sulfate heptahydrate	NaOH	Stirred at 25 °C for 8 h, dried 100 °C 4 h, Calcined 400 °C for 2 h, pH of 11	23.04, 19, 37	XRD, SEM, UV–visible spectrophotometer	Triangular structure, Rod and grain After calcination: flakes like rose petals structure	ZnO nanoparticles synthesized from sulfate precursors were distinct with organized rods- and flowers-like morphology before calcination but the morphology changed after calcination at 400 °C to only flakes type. However, the morphology did not change even after calcinations for the nanoparticles synthesized from other two precursors such as zinc acetate and zinc nitrate	Gopal and Kamila (2017)

Table 6 (continued)

Methods	Zinc salt	Other solvents	Synthesis conditions	Crystallite size (nm)	Characterization techniques	Shape	Research findings	References
Precipitation	Zinc acetate dihydrate, zinc chloride, zinc nitrate hexahydrate	Hexamethylenetetramine $(CH_2)_6 N_4)$	Stirred at 87 °C for 6 h, later oven dried at 80 °C for 7 h	46, 41.3, 40.6	XRD, SEM, EDX, BET	Nanorods, Nanorods, Nanorods	All ZnO samples showed rod-like shape network with difference sizes. When Zinc acetate dihydrate was used as precursor, short rods were formed and while longer nanorods were obtained using Zinc chloride	Perillo et al. (2018)
Precipitation	Zinc nitrate hexahydrate, Zinc chloride	Polyvinylpyrrolidone, NaOH	95 °C for 3 h under stirring, dried in air at 60 °C for 12 h	28, 30	XRD, PL, FT-IR	-	There was a significance difference in the particle size of the ZnO nanoparticle. The authors reported crystallite size of 28 and 30 nm for ZnO nanoparticles prepared using Zn $(NO_3)_2{\cdot}6H_2O$ and $ZnCl_2$, respectively	Mrad et al. (2018)
Sol–gel	Zinc chloride, Zinc nitrate hexahydrate	NaOH	Stirred at 90 °C for 2 h	20, 40			The authors found that the crystallite size is a function of the nature of precursors ($ZnCl_2$ or $Zn(NO_3)_2$ and the synthesis temperature (50 to 90 °C)	Savi et al. (2018)

Table 6 (continued)

Methods	Zinc salt	Other solvents	Synthesis conditions	Crystallite size (nm)	Characterization techniques	Shape	Research findings	References
Green route	Zinc acetate, Zinc nitrate hexahydrate	Fresh leaves of *L. nobilis*	Stirred for 2 h	21.49, 25.26	SEM, EDX, FT-IR, XRD and UV–Visible spectrophotometer	Spherical shape m flower-shape	Spherical and flower shapes of ZnO nanoparticles with the average crystallite size of 21.49, 25.26 nm were produced using Zinc acetate and Zinc nitrate precursors, respectively. Different Zinc precursors exerted slight effect on the crystallites size of the ZnO nanoparticles produced	Fakhari et al. (2019)

The results of different analyses summarized in Table 9 indicate that the surface area of ZnO nanoparticles increases so also the stirring rate and concentration of the zinc precursor, while the surface area reduces as reaction temperature and calcination temperature increase. The results also show that the change in surface area as the synthesis condition changes has little or no effect on the crystal structure of the ZnO nanoparticles produced. The effect of solution pH suggests that large surface area is obtained as the pH approaches a basic medium. The effect of different zinc salt did not have any major effect on the surface area of the ZnO nanoparticles. The next section of the review focuses on the application of ZnO nanoparticles for wastewater treatment.

Water pollution

Water pollution occurs when unwanted materials enter into water bodies, change its quality, and later become harmful to the environment and human health (Alrumman et al. 2016). Water is an important natural resource that needs to be protected against foreign toxic materials (Subramanian 2018). In fact, water pollution is the leading worldwide cause of deaths and diseases more war (Ladu et al. 2018). The discharge of the untreated wastewater into the water bodies has been attributed to the growing number of several diseases such as cholera, typhoid fever among others (Singh et al. 2018). It has been estimated that the world generates more than 5–10 billion tons of industrial wastes, much of which is pumped untreated into rivers, oceans, and other waterways (UNEP-Global. Marine Litter 2020). The wastewater is associated with several pollutants ranging from organic, microbial to inorganic such as heavy metals which include lead (Pb), zinc (Zn), nickel (Ni), arsenic (As), copper (Cu), chromium (Cr), iron (Fe), selenium (Se), vanadium (V), cobalt (Co), cadmium (Cd), and mercury (Hg) as a result of industrial activities (Alalwan et al. 2020). These heavy metals are recognized as a major toxic hazardous material to humans and the aquatic system (Akpor et al. 2014).

Effect of heavy metals and treatment methods

Globally, heavy metals pollution in water has caused serious health effects to humans and the ecosystem since they are non-biodegradable and highly toxic (Ogbomida et al.

2018). These heavy metals are distributed in the environment through natural and anthropogenic activities (Engwa et al. 2016). Exposure to metals such Pb, Zn, Ni, As, Cu, Cr, Fe, Se, V, Co, Cd, and Hg can affect growth and development causing mental disorder, cancer, damage the liver, kidneys, lungs, and in extreme cases, death depending on the exposure dose and time (Monisha et al. 2014). The specific effects of some of the heavy metals have been summarized (see Table10). The possible removal of these pollutants from the wastewater before the discharge to the environment has recently become the focus of many researchers owing to its negative effect on the environment. Effective wastewater treatment is a major prerequisite for a growing economy in the current era of water scarcity. Methods for removing these pollutants from wastewater include chemical precipitation, ion exchange, photocatalytic technology, coagulation, electrocoagulation, membrane bioreactor, flocculation, chemical oxidation and reduction, reverse osmosis, ultrafiltration electrodialysis, and activated carbon adsorption (Abbas et al. 2016). However, the aforementioned methods have some limitations such as sensitive operating conditions, high reagent requirement, low removal efficiency, high cost, and generation of toxic secondary pollutants (Gunatilake 2015). Among the methods used for removal of heavy metals, adsorption technique platform with nanotechnology has been recognized as the most suitable method for removal of heavy metals due to their unique properties which include, low cost, high efficiency, ease of operation, simple design, cost-effective and, regeneration potentials (Cai et al. 2019; Wołowiec et al. 2019). Furthermore, it has been reported that adsorption did not produce secondary pollutants (Gupta et al. 2014). Many materials such as activated carbon from agricultural waste chitosan, clay, polymer biopolymers, graphene-based are known for their efficiency for the removal of heavy metals (Sharma et al. 2017; Maduabuchi 2018). Many other nanoadsorbents developed include metal oxide nanoparticles such as zinc oxide, ferric oxides, magnesium oxides, titanium oxides, manganese oxides, silicon oxides, cerium oxides, and aluminum oxides nanoparticles, nanocomposites and rubber tire, multiwalled carbon nanotubes, carbon nanotubes (Ihsanullah et al. 2015; Mahmoodian et al. 2015). Among the aforementioned, metal oxides such as ZnO have been widely recognized as a suitable nanostructure material that can solve the deficiencies associated with many adsorbents. Zinc oxide is the most popular due to its excellent properties such as high surface area, easy removal after sorption, and pronounced selectivity of pollutants at trace concentrations, antimicrobial activities, nontoxicity, and simple synthetic methods among others metal oxide nanoparticle (Kumar et al. 2013). ZnO nanoparticles have been the major focus of many researchers as a new adsorbent that could be used to remove heavy metals from industrial wastewater due to its exceptional chemical and thermal resistance and others (Gupta et al. 2014).

Adsorption technology

Adsorption is a mass transfer process that involves accumulation of substances at the interface between two phases, such as liquid–solid, liquid–liquid, liquid–gas, and solid–gas interface and becomes bound by physical or chemical interaction (Girish and Murty 2017). Adsorption is an effective and inexpensive process used for the treatment of wastewater (Lata et al. 2019). The removal of pollutants usually occurs when an adsorbate in a solution comes into contact with the adsorbent, concentrates or accumulates on another surface as shown in VIII. Adsorption process is often reversible, since the adsorbents can be regenerated by desorption process (Cai et al. 2019). Adsorption can be classified into physical adsorption (physisorption) and chemical adsorption (chemisorption) and depend on the properties of both the adsorbate and the adsorbent (Ziółkowska et al. 2016). An adsorbent material must have certain important properties, such as high surface area, the distribution of pores, and the existence of the pores that have a significant influence on the form of the adsorption process, high internal volume accessible to the various target components (Kyzas and Kostoglou 2014). If the forces of attraction that exist between adsorbate and adsorbent have a physical nature, the process is called physisorption. This process is characterized by the formation of weak intermolecular forces such as van der Waals forces, reversible process, and formation of multilayer of adsorbate on the adsorbent, decrease with increase in temperature

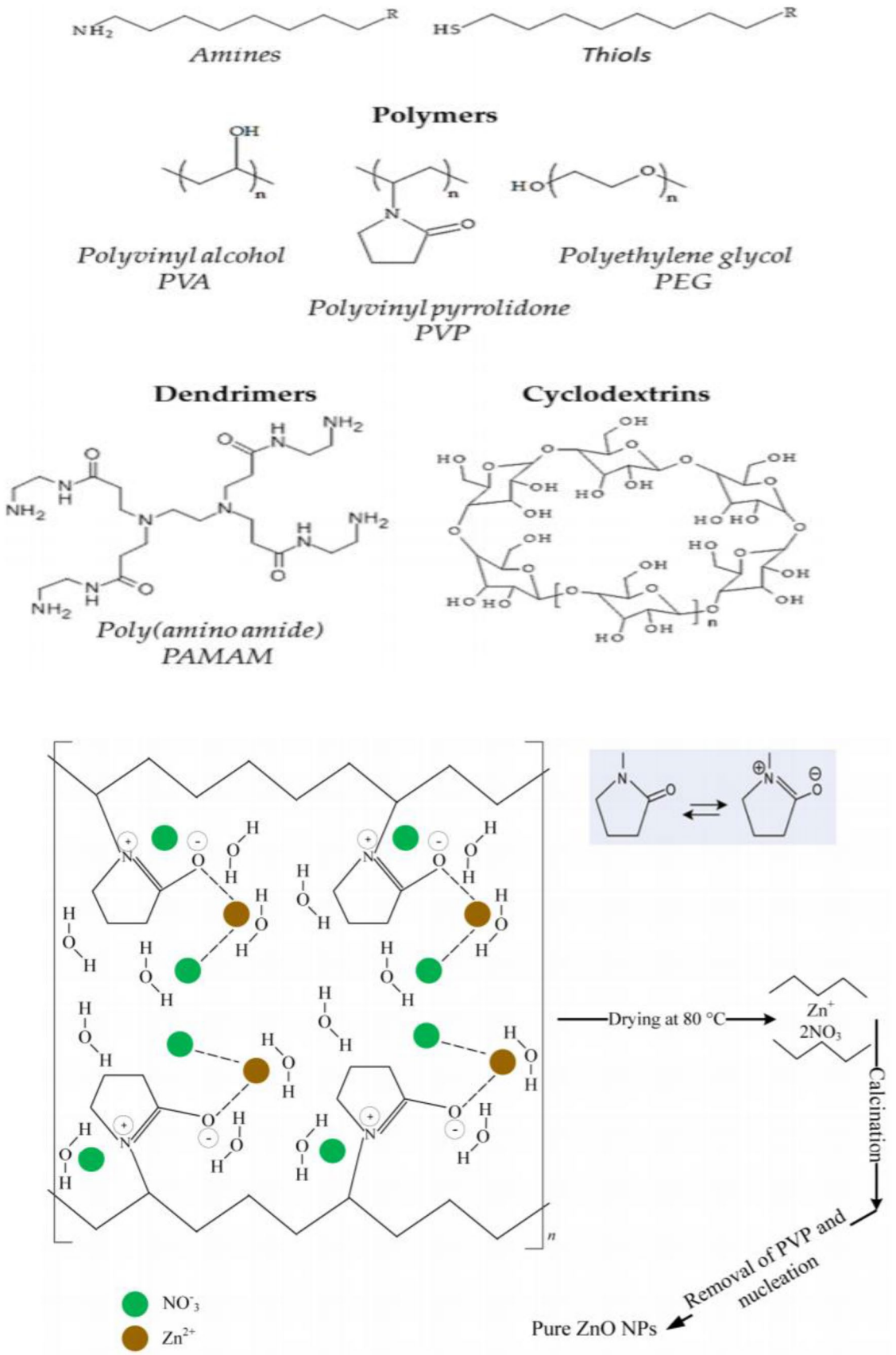
Amines
Thiols
Polymers
Polyvinyl alcohol
PVA
Polyvinyl pyrrolidone
PVP
Polyethylene glycol
PEG
Dendrimers
Poly(amino amide)
PAMAM
Cyclodextrins
Drying at 80 °C
Calcination
Removal of PVP and nucleation
Pure ZnO NPs
NO3-
Zn2+

◂**Fig. 4** Selected capping agents used in synthesis of ZnONPs, possible mechanism of formation of ZnO nanoparticles using plant Extract (**a**) and a proposed mechanism of the interaction between zinc ions (Zn^{+}) and polyvinyl pyrrolidone (PVP) (**b**)

and has a low enthalpy of adsorption. On the other hand, if the interaction between the adsorbent and adsorbate has a chemical nature, the process is known as chemisorption, thus resulting to the formation of a strong chemical bond (Abas et al. 2013). The chemisorption process is characterized by the formation of a monolayer of adsorbate on the adsorbent, has a high enthalpy of adsorption and can take place at all temperatures and in most cases not reversible (see Fig. 6).

Mechanisms of adsorption technology

The mechanism of adsorption involves the sorption of sorbate molecules on the surface of the sorbent through molecular interactions, and diffusion of sorbate molecules from the surface into the interior of the sorbent materials, either by monolayer or multilayer (Bushra et al. 2017). Adsorption process involves the binding of metal ions by physical (van der Waals forces) or chemical (ion exchange, chelation, precipitation, binding, complexation, and reduction). Various factors such as the nature of adsorbent, temperature, dosage, adsorption time, the reaction temperature, and the surface area played an important role in the removal of heavy metals by ZnO nanoparticle (Iftekhar et al. 2018). The adsorption of heavy metals from wastewater using ZnO nanoparticles could be complex depending on the nature of capping agents used during the synthesis of ZnO nanoparticles, because the capping agent may contain different functional groups that may greatly influence the removal of the heavy metals through metal ion exchange, chelation, precipitation, binding, complexation, and reduction (see Fig. 7.). The adsorption process may be simple or complex depending on the number of contaminants in the aqueous matrix. There are instances where the adsorption process may contain one, two, three or more pollutants in the wastewater and in most cases serious competition for the active surface sites among the adsorbates becomes an issue. The selectivity factor for the adsorbents also comes into play and may be in the form of electrostatic repulsion (desorption) or electrostatic attraction (adsorption) between the adsorbate and adsorbents.

Physical adsorption (physisorption) is the simplest immobilization method; it occurs when the attractive forces present between adsorbate and adsorbent are weak such as van der Waals forces, hydrophobic interactions, and hydrogen bonding (Sandhyarani 2019). This process occurs readily at low temperatures and decreases with increasing temperature. Physical adsorption has been reported to have a low enthalpy of adsorption (< -40 kJ/mol) with a multilayer adsorbate on adsorbent (Chakraborty et al. 2009). Chemical Adsorption (chemisorption) involves a chemical reaction between the adsorbent and adsorbate and usually leads to chemical bond formation and have a higher enthalpy of adsorption in the range of 80–240 kJ/mol (Mahmoud 2015).

Zinc oxide Nanoparticles as Nano-adsorbent for removal of heavy metals from aqueous matrix

Different researchers have employed ZnO nanoparticles to remove heavy metals from simulated and industrial wastewater. For instance, Mahdavi et al. (2012) investigated the removal of Cd^{2+}, Cu^{2+} Ni^{2+}, and Pb^{2+} from aqueous solutions using ZnO nanoparticles as an adsorbent. The XRD result in the ZnO nanoparticles revealed a crystallite size of 16.70 nm while SEM analysis confirmed the formation of rod-like shape with a crystallite size of 25 nm. The BET analysis of the revealed specific surface area, total pore volume, and pore size of 31.20 m^2/g, 12.09, and 15.81 nm, respectively. The authors found that the adsorption of the heavy metal ions increases as the pH of the solution increases from acidic to alkaline. It was noticed that the pH of the solution played an important role in the adsorption of heavy metals by nanoadsorbents. This is expected because, at lower pH (acidity conditions), the hydrogen ions strongly compete with heavy metal ions in the solution (Ouyang et al. 2019). Moreover, the authors also observed that an increase in the absorbent dose (0.5 to 5 g/l) resulted to an increase in the removal efficiency of Cd^{2+}, Cu^{2+}, Ni^{2+} and Pb^{2+} with Pb^{2+}, having the highest percentage removal of 81.5% at a dosage of 5 mg/g. The observed trend was attributed to the increase in the number of binding sites as

Table 7 Effect of variation of concentration of zinc salt precursors with sodium hydroxides on the nature of ZnO nanoparticles

Methods	Precursor zinc salts	Other solvents	Concentration (M)	Reaction condition	Crystallite size (nm)	Characterization techniques	Shape	Research findings	References
Hydrothermal	Zinc acetate dihydrate	NaOH	0.05, 0.1	Dried 90 °C for 2 h	54, 75	XRD, SEM	Platelets and flaky-like network (0.05 M), nanotubes, spherical and nanorods (0.1)	The results indicated that the higher the concentration of precursor, the smaller the average crystallite size of ZnO nanopowder	Osman and Mustafa (2015)
Precipitation	Zinc acetate dihydrate	NaOH	0.1, 0.2, 0.3 to 0.4	90 °C for 2 h	40, 38, 30, 23	XRD, SEM, RS, PL	Spherical	The authors reported the reduction of crystallite size as the concentration of the NaOH to zinc acetate dihydrate increases	Koutu et al. (2016)
Green route	Zinc nitrate hexahydrate	Cherry fruit extract	0.005, 0.02, 0.05 and 0.3	pH of 8, temperature stirred at 25 °C and for 12 h	20.7–96.5	XRD, SEM,FTIR, UV–Visible spectrophotometer	Spherical	The authors found that the optimum conditions for the synthesis of ZnO nanoparticles were 0.005 M of zinc nitrate at pH of 8, 25 °C and 12 h	Mohammadi and Ghasemi (2018)
Precipitation	Zinc nitrate hexahydrate	Poly- PVA	1.89, 2.27, 3.34	70 °C under suitable magnetic stirring for 2 h allowed to dry in an oven at 160 °C for 12, hours, stirred by magnetic stirrer for 15 min	19, 22, 24	XRD, SEM, FTIR, UV–Vis	Spherical	The authors found that the crystallite size of the ZnO nanoparticles increases as the concentration of PVA concentration increased	Belay et al. (2018)
Green route	Zinc nitrate hexahydrate	NaOH *A. lebbeck*	0.1, 0.05, 0.01	Stirring at 60 °C for 5 h, calcined at 350 °C ± 10 °C for 2 h	66.25, 82.52, 112.87	UV–visible spectrophotometer, FTIR, XRD, SEM, EDX	Irregular spherical	The authors revealed the increase of crystallite size of ZnO nanoparticles as the concentration of zinc nitrate hexahydrate decreases	Umar et al. (2019)

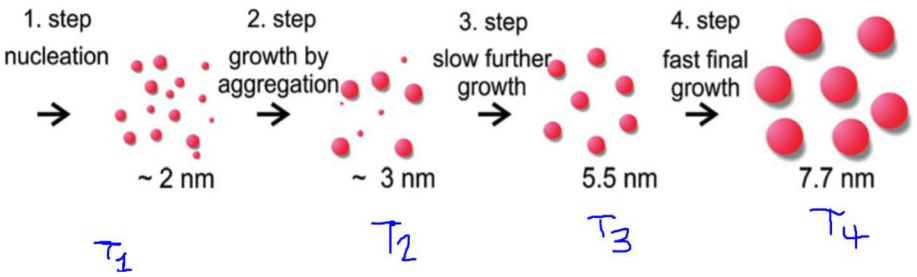

Fig. 5 Schematic illustration for effect of reaction time on the synthesis of ZnO nanoparticles (Polte et al. 2010)

the nanoabsorbents increase (Xie et al. 2015). The maximum removal efficiency was achieved for all the four ions after 180 min and there was no significant increase in the removal efficiency of the metal ions after 180 min to 24 h. The maximum uptake of the metal ions was reported to be 114.5 mg/g. In addition, Salmani et al. (2013) reported removal efficiency of 89.6% for Cd^{2+}ion using ZnO nanoparticles. The authors found that the Cd^{2+} ion removal followed the pseudo-second-order and Langmuir isotherms model and the efficiency was highly sensitive to the change in pH and ionic strength. They also confirmed that removal efficiency increases as the pH of the solution increases from 4 to 7. The result showed that the maximum removal of Cd^{2+}ion was achieved at lower contact time and later decrease despite increase in the contact time. This shows that the solution pH, contact time, concentration of metal, and temperature affect the removal of metal ions using ZnO nanoparticle as an adsorbent. Moreover, other works done by various researchers on the application of ZnO nanoparticles as a nanoadsorbent for the removal of heavy metals from wastewater is presented in Table 10

Table 11 shows ZnO nanoparticle of different sizes and morphologies were synthesized by different methods. The result revealed that the ZnO nanoadsorbents show adsorptive removal efficiency between 61 and 100% with ZnO nanoparticle with a spherical shape has the highest (100%) removal for Cu^{2+}. From the Table 11, Bi^{3+} has the lowest adsorption using spherical ZnO nanoparticles. The adsorptive capacities of ZnO nanoparticles depend majorly on several factors particularly the methods of synthesis which have direct link to the textural, morphology and optical properties of the material under review.

Effect of solution pH on removal efficiency of heavy metals

pH is one of the most significant control factors that directly influence removal of heavy metals during adsorption process. It can also influence the binding sites on the surface of the nanoadsorbent and also affect the degree of heavy metals ionization and chemical nature of the adsorbent (Jin et al. 2011; Duan et al. 2016). For instance, Degen and Kosec (2000) studied the effect of pH on the removal of heavy metals from an electroplating wastewater using ZnO nanoparticles as an adsorbent and found that at a pH below 7 (acidic), the solution was highly protonated (H^+) resulting in a high positive surface charge on the surface of the adsorbent which repels the positively charged metal ions and subsequently low removal efficiency. However, due to dominant hydroxide ions (OH^-) at a pH greater than 7, the adsorbent surface becomes negatively charged resulting to a high negative charge density that attracts more metal ions (see Fig. 8) They also reported that at a pH above 6, there is possibility that the metals could precipitate to form hydroxides as a result, the adsorption process is hindered. Furthermore this trend

Table 8 Effect of reaction time on the nature of ZnO nanoparticles

Methods	Precursor zinc salt	Other chemicals	Time	Other reaction condition	Crystallite size (nm)	Shape	Characterization techniques	Research outcome	Reference
Hydrothermal	Zinc acetate dehydrate	Hydrazine hydrate, ammonia	10 to 15	Calcination time of 2 h	50–150	Needle and flower like	SEM, TEM, XRD	The crystallite size increases as the nucleation time increases	Hasanpoor et al. (2015)
Co-precipitation	Zinc acetate dihydrate	Methanol, potassium hydroxide	0, 2, 8 min	Stirred for 2.5 h, dried in the oven at 60°C for 8 h and calcined at 350 °C for 2 h	41, 84, 135	Nearly Spherical	SEM, XRD, FTIR, UV–Visible spectrophotometer	The crystallite size increases as the nucleation time increases	Manzoor et al. (2015)
Sol–gel	Zinc acetate dihydrate	Methanol, NaOH	12, 24 h	pH 9, dried under room temperature	49 and 200	Nanorods	SEM and XRD	The crystallite increases as the nucleation time increases	Harun et al. (2016)
Green route	Zinc acetate dihydrate	*Pichia kudriavzevii* Yeast Strain	12, 24, 36 h	Stirred at room temperature	11.25, 38.48 and 54.27	Spherical	XRD, TEM, PL, FTIR, UV–Visible spectrophotometer	The reaction duration was found to play a critical role in the size, shape and distribution of ZnO nanoparticles	Moghaddam et al. (2017)
Sol–gel	Zinc acetate	NaOH	4, 6, 8 h	Stirred for 2 h, dried 100°C for 2 h	33.32,35.57, 38.40 and 42.63	Nanorods	XRD, FTIR, SEM, UV–Visible spectrophotometer and PL	The authors found that the crystallite size increases as the nucleation time increases	Shaikh and Ravangave (2015)

Table 9 Effect of reaction temperature on the properties of ZnO nanoparticles

Methods	Precursor zinc salt	Crystal structure	Surface area (m^2/g)	Total pore volume	Reaction condition	Crystallite size (nm) (m^3/g)	Research findings	References
Precipitation	zinc acetate	Hexagonal wurtzite	8, 10.8, 12.0, 23	0.006, 0.008, 0.009, 0.015	Synthesized at different zinc concentration (0.9, 1.4, 1.9 M)	53.7, 63.8, 66.5 and 41.3	The studied indicates that an increase in zinc acetate concentration increases the surface area of the ZnONPs produced under potassium hydroxide and sodium hydroxides as precipitating agents	Kołodziejczak-Radzimska et al. (2012)
Precipitation	zinc acetate	hexagonal wurtzite	19.1, 18.2,	0.025,0.022	Stirred at 150 rps with 0.3 M precursor concentration	32 to 57	As the temperature increases from 50 to 90 the surface area and the pore volume decreases and the structure changes from rod-like to flowers-like structure	Pushpanathan et al. (2012a)
Sol–gel	Zinc acetate dihydrate	hexagonal wurtzite	15 to 53 m^2/g	0.00041, 0.0021, 0.0013, 0.0012, 0.0018	0.1 M of Zinc precursor was used, synthesized at different pH (8, 9, 10, 11 and 12), stirrer at 400 rpm under temperature of 70℃ for 1 h	24.65, 31.70, 48.09, 65.51, 53.15	The authors fund that the pH of 8 give the highest surface area	Abdol-Aziz et al. (2018)
Precipitation	zinc acetate	hexagonal wurtzite	22.9 to 2.6	40–60	Stirred for 30 min and sonicated for 15 min at 0.1 M, dried at 70 °C for 18 h, calcined at different temperature (300 °C, 400 °C, 500 °C, and 600 °C) for 4 h	3, and 25	It was reported that as the calcination temperature increases from 400 °C-600°C the surface area decreases from 22.9 to 2.6 and the structure remained unchanged	Baharudin et al. (2018)

Table 9 (continued)

Methods	Precursor zinc salt	Crystal structure	Surface area (m^2/g)	Total pore volume	Reaction condition	Crystallite size (nm) (m^3/g)	Research findings	References
Hydrothermal	hydrozincite		39.1, 27.2, 17.1, 7.2, 2.1	48, 35, 23, 2	Synthesized at room temperature, ZnONPs were oven dried at different temperature (110, 200, 400, 600, 800) for 48 h	12, 29, 35, 45, 64	The researchers concluded that as the different drying temperature increases the surface area of the ZnONPs produced decreases	Rezende et al. (2009)
Sol–gel	zinc nitrate hexahydrate		0.12, 0.20, 0.13, 0.23	-	Stirred for 24 h 70 °C dried for r 3 days at 12 °C	74.9, 70.5, 74.8, 74.8	The authors fund that by raising the stirring time from 1 to 24 h the surface area increases from 0.12 to 0.23 m^2/g	Alnarabiji et al. (2014)
Precipitation	Zinc acetate dihydrate, zinc chloride, zinc nitrate hexahydrate	Hexagonal wurtzite	2.01, 3.09, 7.91	0.0021, 0.0097, 0.012	Synthesized at 87 °C for 6 h with 0.01 M concentration	46, 41.3, 40.6	The studied indicated that different salt precursor give different surface area and pore volume	Perillo et al. (2018)
Sol–gel	Zinc acetate	hexagonal geometry	50.41, 151.1, 143.5, 578, 126, 136.5, 130.2, 133.3	13.43, 8.02, 7.22, 9.80, 7.43, 7.62, 7.50, 8.38	0.15, 0.2, 0.25, 0.3, 0.35, 0.4, 0.45, and 0.5 M	Stirred at room temperature for 12 h using different concentration (26.73, 36.73, 28.61, 35.12, 32.51, 27.35, 35.01, 23.14) and calcined at 400 °C for 30 min	It is found that with an increase in NaOH concentration, the specific surface area initially increases. At optimal NaOH concentration, the surface area unexpectedly increases and then decreases with increased NaOH concentration	Jadhav et al. (2014)

Table 10 The MCL standards for the most hazardous heavy metals. *Source*: Babel and Kurniawan (2003)

Heavy metal	Toxicities	MCL (mg/l)
Arsenic	Skin manifestations, visceral cancers, vascular disease	0.05
Cadmium	Kidney damage, renal disorder, human carcinogen	0.01
Chromium	Headache, diarrhea, nausea, vomiting, carcinogenic	0.05
Copper	Liver damage, Wilson disease, insomnia	0.25
Nickel	Dermatitis, nausea, chronic asthma, coughing, human carcinogen	0.2
Lead	Damage the fetal brain, diseases of the kidneys, circulatory system, and nervous system	0.006
Mercury	Rheumatoid arthritis, and diseases of the kidneys, circulatory system, and nervous system	0.00003

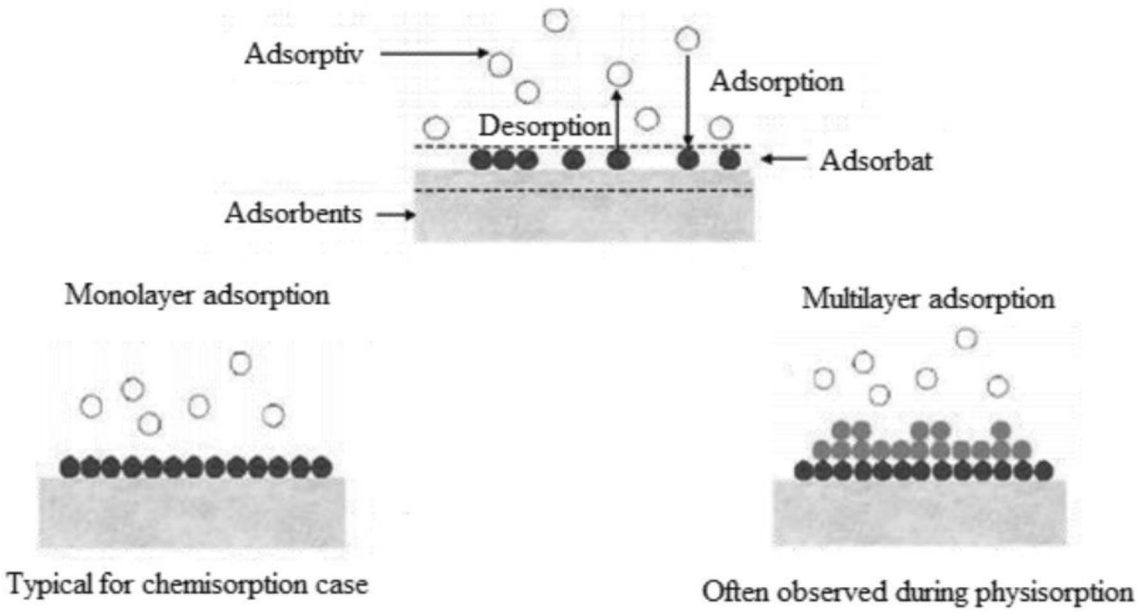

Fig. 6 Adsorption process and adsorption types created based on research by Christmann (2010)

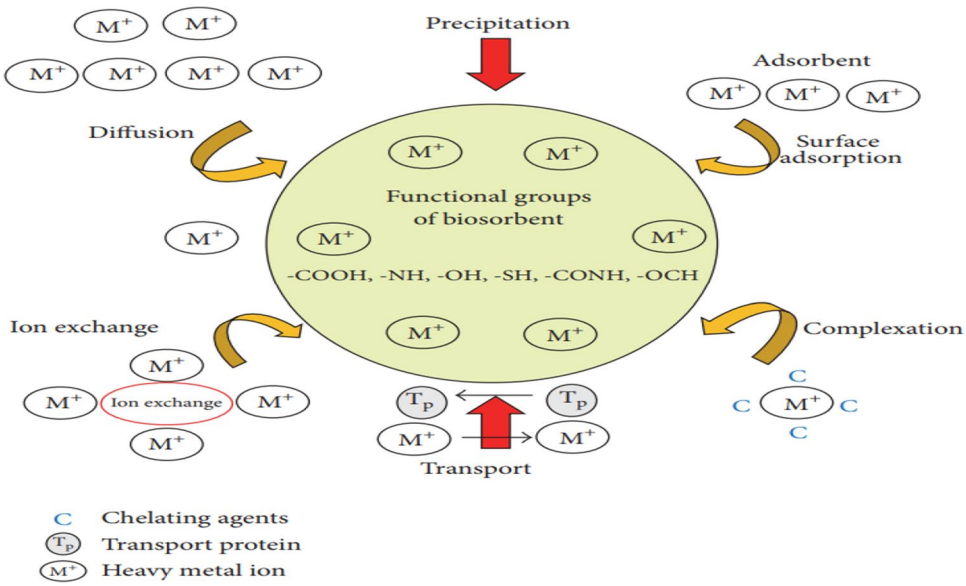

Fig. 7 Adsorption mechanisms created based on research by Mathew et al. (2016)

Table 11 Summary of ZnO nanoparticles as nanoadsorbent for the removal of heavy metals from aqueous matrix

Methods	Characterization techniques	Shape	Crystallite size (nm)	Pollutant(s)	Removal (%)/ adsorption capacity (mg/g)	Other adsorption conditions	Research findings	References
Sol–gel	SEM, EDS, BET, TEM, FT-IR, XRD, DTA and TGA	Spherical	8	Pb^{2+}, Hg^{2+}, Cd^{2+} Bi^{3+}	97.1, 86.8, 80.9, 61.2	Contact time (60 min), Dosage (0.250 g), temperature (30 °C), metal ions concentration at 0.01 M	The maximum adsorption capacity of Pb^{2+} 8.768 mg/g with highest removal of 97.1%	Angelin et al. (2015)
Precipitation	FT-IR, XTD, TGA-DTG, SEM, and TEM	Flaky fibrous structure shaped	31	Cr (VI)	120.92	Dosage (1 g), temperature (30 °C)	The authors reported that the maximum adsorption capacity for removal of chromium was 120.92 mg/g. The reaction followed the second-order kinetics and chemisorption is the rate-determining step	Ahmad (2015)
Precipitation	FTIR and TEM analysis	Spherical	38- 45	Cr (VI)	96	Contact time (210 min), pH of 2.5, temperature (60 °C), dosage (0.5 g)	The maximum adsorption of Cr (VI) ions using adsorbent was achieved within 210 min	Ahmed and Yousef (2015)
Hydrothermal	SEM and XRD	Pinecone like	30		142.56	pH range of 5.6 at temperature of 298 K	The maximum adsorbed amounts of Cr (VI) adsorbed was high at 298 K, high maximum adsorbed amounts of Cr (VI), being 14 2.56 mg/g	Ma et al. (2016)
Precipitation	FTIR, SEM, FTIR and TGA	Spherical	73	Cu^{2+}, Pb^{2+}, Cd^{2+}	100, 77.47, 97.85	Stirred at 120 rpm at 30 °C for 150 min, adsorbent dosage (0.1 g)	Optimal conditions were observed at solution pH 8. The reaction fitted to Pseudo-second order kinetic	Anusa et al. (2017)

Table 11 (continued)

Methods	Characterization techniques	Shape	Crystallite size (nm)	Pollutant(s)	Removal (%)/ adsorption capacity (mg/g)	Other adsorption conditions	Research findings	References
Green	XRD TEM, and UV–vis	Regular hexagonal surface shape	10.01 2.6	Pb(II)	93.00	pH of 5, temperature of 70^0C	The maximum removal efficiencies were 93% at pH 5. The excellent efficiency of the as-synthesized ZnO nanoparticles made it suitable for the removal of heavy metals from aqueous system	Azizi et al. (2017)
Precipitation	XRD, TEM and DLS	Spherical	10–11 nm	Cd(II)	98.71	Dosage(120 mg), volume of aqueous solution (10 ml), pH (5), contact time (20 min) and initial heavy metal ion concentration (300 mg/l)	The maximum removal efficiencies were achieved at solutions pH of 5 and at initial heavy metal ion concentration of 300 mg/l. Adsorption isotherm studies indicated that the data fitted well to the Freundlich isotherm model	Nalwa et al. (2017)
Precipitation	XRD, FT-IR spectroscopy, SEM, and TGA	ZnO nanorods	_____	As(III)	96	pH (7), dosage (0.4 contact time (105 min), temperature (323 K)	The results revealed that the pseudo-second-order kinetic model best described the data. The maximum As(III) sorption capacity of ZnO nanorods was found to be 52.63 mg/g at pH 7, adsorbent dose 0.4 g, contact time 105 min, and temperature 323 K	Yuvaraja et al. (2018)

Table 11 (continued)

Methods	Characterization techniques	Shape	Crystallite size (nm)	Pollutant(s)	Removal (%)/ adsorption capacity (mg/g)	Other adsorption conditions	Research findings	References
Precipitation	XRD, SEM and EDX	Nanorods arranged like flower		Cr(VI)	98	40 min with optimum value of pH 3	The amount of chromium adsorption increases with increase in adsorbent dosage, whereas the adsorption was maximum in the first 40 min with optimum pH of 3. The morphology of ZnO nanorods changes into nanosheets after adsorption process	Kamath et al. (2018)

showed that electrostatic interaction played a major role in the removal of heavy metals.

Conclusion

In summary, the effects of different synthesis parameters on the textural, optical and microstructural properties of ZnO nanoparticles have been provided. The adsorptive behaviour of ZnO nanoparticles for the removal of heavy metals especially at different solution pH has also been summarized. Based on the review, the following conclusions were drawn. Acidic medium favoured the formation of smaller size of ZnO nanoparticles compared to alkaline medium. Several reports indicated a decrease in the crystallite size of ZnO nanoparticles as the pH increases from 7 to 12. Reaction time, reaction temperature and calcination temperatures influenced the crystallite size of ZnO nanoparticles. Different zinc salts have little effect on the crystallite size but exerted greater influence on the morphology of the ZnO nanoparticle produced. The concentration of the zinc precursor shows increases in the crystallite size at a higher concentration of zinc in the solution. These findings indicated that these factors strongly affect the crystallite size and the morphology of the zinc oxide nanoparticles. The crystallite sizes with respect to each parameter also depend on the methods of synthesis of ZnO nanoparticles. There are still divergent views as reported by the researchers on the increase and decrease in the particle size of the ZnO nanoparticle. The mechanisms of the increase or decreases in the crystallite size with respect to the variations of solution pH, synthesis temperature, different salt precursor, and synthesis time are not clearly understood and still require further investigation. Optimization of all these parameters should be carried out to fully understand the mechanism of the synthesis of ZnO nanoparticles. Regeneration of the ZnO should be performed to evaluate the cost effectiveness of ZnO as an adsorbent. Future research should focus on the immobilization of ZnO nanoparticles on suitable supports for easy separation after usage.

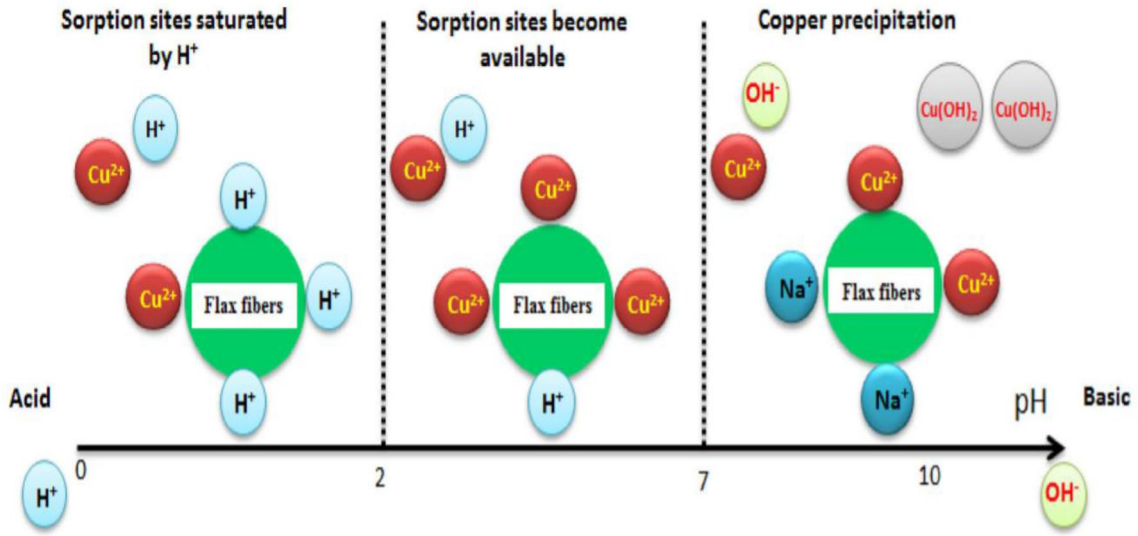

Fig. 8 Effect of pH on the adsorption of heavy metals created based on research by Abbar et al. (2017)

Abbreviations

AFM	Atomic force microscopy
BET	Brunauer, Emmett and Teller
DRS	Diffuse reflection spectroscopy
EDS	Dispersive X-ray analysis
FDA	Food and Drug Administration
FESEM	Field emission scanning electron microscopy
FT-IR	Fourier-transform infrared spectroscopy
HRTEM	High-resolution tunneling microscope
MCL	Maximum contaminated level
PL	Photoluminescence
PVA	Polyvinyl alcohol
PVP	Polyvinyl pyrrolidone
RS	Raman spectroscopy
SEM	Scanning electron microscopy
TEM	Transmission electron microscope
UV–vis	Ultraviolet–visible spectroscopy
XRD	X-ray powder diffraction
DLS	Dynamic light scattering
AFM	Atomic force microscopy analysis

Funding The author(s) received no specific funding for this work.

Compliance with ethical standards

Conflict of interest The authors declare that they have no conflict of interest.

Ethical standards The study did not include human or animal subjects; therefore ethical approval is not required.

References

Abas SNA, Ismail MHS, Kamal ML, Izhar S (2013) Adsorption process of heavy metals by low-cost adsorbent: a review. World Appl Sci J 28:1518–1530. https://doi.org/10.5829/idosi.wasj.2013.28.11.1874

Abbar B, Alema A, Marcotte S, Pantet A, Ahfir N, Bizet L, Duriatti D (2017) Experimental investigation on removal of heavy metals (Cu^{2+}, Pb^{2+}, and Zn^{2+}) from aqueous solution by flax fibres. Process Saf Environ Prot 109:639–647

Abbas A, Al-Amer AM, Laoui T, Al-Marri MJ, Nasser MS, Khraisheh M, Atieh MA (2016) Heavy metal removal from aqueous solution by advanced carbon nanotubes: critical review of adsorption applications. Sep Purif Technol 157:141–161. https://doi.org/10.1016/j.seppur.2015.11.039

Abdol-Aziz RA, Abd-Karim SF, Rosli NA (2018) The effect of pH on zinc oxide nanoparticles characteristics synthesized from banana peel. Key Eng Mater 797(271):279

Abdullah AK, Awad S, Zaraket J, Salame C (2017) Synthesis of ZnO nanopowders by using sol gel and studying their structural and electrical properties at different temperature. Energy Procedia 119:565–570. https://doi.org/10.1016/j.egypro.2017.07.080

Ahmad R (2015) Polyaniline/ZnO nanocomposite: a novel adsorbent for the removal of Cr(vi) from aqueous solution advances in composite materials development, pp 1–23. https://www.intechopen.com/books/advances-in-composite-materials-development/polyaniline-zno-nanocomposite-a-novel-adsorbent-for-the-removal-of-cr-vi-from-aqueous-solution. Accessed 13 Dec 2019

Ahmadivand A, Karabiyik M, Pala N (2016) Plasmonic photodetectors. Photodetectors. https://doi.org/10.1016/b978-1-78242-445-1.00006-3

Ahmed NMP, Yousef NS (2015) Synthesis and characterization of zinc oxide nanoparticles for the removal of Cr (VI) International. J Sci Eng Res 65:1235–1243

Akpor OB, Otohinoyi DA, Olaolu TD, Aderiye BI (2014) Pollutants in wastewater effluents: impacts and remediation processes. Int J Enviro Res Earth Sci 3(3):50–59

Alalwan HA, Kadhom MA, Alminshid AA (2020) Removal of heavy metals from wastewater using agricultural by products. J Water Supply Res Technol AQUA 692:99–112. https://doi.org/10.2166/aqua.2020.133

Alami ZY, Salem M, Gaidi M, Elkhamkhami J (2015) Effect of Zn concentration on structural and optical proprieties of ZnO thin films deposited by spray pyrolysis. Adv Energy Int J: AEIJ 2(4):11–24. https://doi.org/10.5121/aeij.2015.2402

Al-Hada NM, Saion EM, Shaari AH, Kamarudin MA, Flaifel MH, Ahmad HS, Gene SH (2014) A facile thermal-treatment route to synthesize ZnO nanosheets and effect of calcination temperature. PLoS ONE 9(8):103–134. https://doi.org/10.1371/journal.pone.0103134

Aljawfi RN, Alam MJ, Rahman F, Ahmad S, Shahee A, Kumar S (2020) Impact of annealing on the structural and optical properties of ZnONPs and tracing the formation of clusters via DFT calculation Arabian. J Chem 13:2207–2218. https://doi.org/10.1016/j.arabjc.2018.04.006

Alnarabiji MS, Yahya N, Abd-Hamid SB, Azizi K, Kashif M, Qureshi S, Alqasem B (2014) The role of surface area of ZnO nanoparticles as an agent for some chemical reactions. Defect Diffus Forum 354:201–213. https://doi.org/10.4028/www.scientific.net/DDF.354.201

Alrumman SA, El-kott AF, Keshk SMAS (2016) Water pollution: source and treatment. Am J Environ Eng 6(3):88–98. https://doi.org/10.5923/j.ajee.20160603.02

Al-Sarraf RAH, Khodair ZT, Manssor MI, Abbas RAA, Shaban AH (2018) Preparation and characterization of ZnO nanotripods and nanoflowers by atmospheric pressure chemical vapor deposition (APCVD) technique. AIP Conf Proc 1968:030005. https://doi.org/10.1063/1.5039192

Alwan RM, Kadhim QA, Sahan KM, Ali AR, Mahdi RJ, Kassim NA, Jassim AN (2015) Synthesis of zinc oxide nanoparticles via sol–gel route and their characterization. Nanosci Nanotechnol 5(1):1–6. https://doi.org/10.5923/j.nn.20150501.01

Ambika S, Sundararajan M (2015) Green biosynthesis of ZnONPs using *Vitex negundo* L. extract: spectroscopic investigation of interaction between ZnONPs and human serum albumin. J Photochem Photobiol B 149:143–148. https://doi.org/10.1016/j.jphotobiol.2015.05.004

Angelin KB, Siva S, Kannan RS (2015) ZINC oxide nanoparticles impregnated polymer hybrids for efficient extraction of heavy metals from polluted aqueous solution. Asian J Sci Technol 6(12):2139–2150

Anusa R, Ravichandran C, Sivakumar EKT (2017) Removal of heavy metal ions from industrial waste water by nano-ZnO in presence of electrogenerated Fenton's reagent. Int J ChemTech Res 10(7):501–508

Ashaf R, Riaz S, Kayani ZN, Naseem S (2015) Effect of calcination on properties of ZnONPs. Mater Today Proc Part B 2(10):5468–5472. https://doi.org/10.1016/j.matpr.2015.11.071

Azhar NEZ, Shariffudin SS, Salman MR, Alrokayan AH, Haseeb AK (2017) Investigation of ZnO nanotetrapods at different evaporation temperatures by thermal-CVD method for OLED applications. J Mech Eng 1(19):1–19

Aziz WJ, Jassim HA (2018) A novel study of pH influence on Ag nanoparticles size with antibacterial and antifungal activity using green synthesis. World Sci News 97:139–152

Azizi S, Shahi MM, Mohamad R (2017) Green synthesis of zinc oxide nanoparticles for enhanced adsorption of lead ions from aqueous solutions: equilibrium, kinetic and thermodynamic studies. Molecules 22(6):831. https://doi.org/10.3390/molecules22060831

Babel S, Kurniawan TA (2003) Low-cost adsorbents for heavy metals uptake from contaminated water: a review. J Hazard Mater 97(1):19–243. https://doi.org/10.1016/S0304-3894(02)00263-7

Baharudin KB, Abdullah N, Derawi D (2018) Effect of calcination temperature on the physicochemical properties of zinc oxide nanoparticles synthesized by coprecipitation. Mater Res Express. https://doi.org/10.1088/2053-1591/aae243

Bakshi MS (2015) How surfactants control crystal growth of nanomaterials. Cryst Growth Des 16(2):1104–1133

Bala N, Saha S, Chakraborty M, Maiti M, Das S, Basu R, Nandy P (2015) Green synthesis of zinc oxide nanoparticles using *Hibiscus subdariffa* leaf extract: effect of temperature on synthesis, anti-bacterial activity and anti-diabetic activity. RSC Adv 5(4993):4993–5003. https://doi.org/10.1039/c4ra12784f

Barhoum A, Rahier H, Benelmekki M, Assche GV (2018) Recent trends in nanostructured particles: synthesis, functionalization, and applications. Fundam Nanopart. https://doi.org/10.1016/b978-0-323-51255-8.00024-0

Basri HH, Talib RA, Sukor R, Othman SH, Ariffin H (2020) Effect of synthesis temperature on the size of ZnONPs derived from pineapple peel extract and antibacterial activity of ZnO–starch nanocomposite films. Nanomaterials 10:1061. https://doi.org/10.3390/nano10061061

Belay A, Bekele B, Chandra RAR (2018) Effects of temperature and polyvinyl alcohol concentrations in the synthesis of zinc oxide nanoparticles. J Nanotechnol Mater Sci 5(1):44–50. https://doi.org/10.15436/2377-1372.18.1946

Belver G, Bedia J, Gómez-Avilés A, Peñas-Garzón M, Rodriguez JJ (2019) Semiconductor photocatalysis for water purification. Nanoscale Mater Water Purif. https://doi.org/10.1016/B978-0-12-813926-4.00030-6

Bettini S, Pagano R, Valli L, Giancane G (2016) Enhancement of open circuit voltage of a ZnO-based dye-sensitized solar cell by means of piezotronic effect. Chem Asian J 11(8):1240–1245. https://doi.org/10.1002/asia.201501325

Buazar F, Bavi M, Kroushawi F, Halvani M, Khaledi-Nasab A, Hossieni SA (2016) Potato extract as reducing agent and stabiliser in a facile green one-step synthesis of ZnONPs. J Exp Nanosci 11(3):175–184. https://doi.org/10.1080/17458080.2015.1039610

Bushra R, Ahmeda A, Shahadat M (2017) Mechanism of adsorption on nanomaterials, pp 90–111. https://www.researchgate.net/publication/310771898_Mechanism_of_Adsorption_on_Nano_materials

Cai Y, Liu L, Tian H, Yang Z, Luo Z (2019) Adsorption and desorption performance and mechanism of tetracycline hydrochloride by activated carbon-based adsorbents derived from sugar cane bagasse activated with ZnCl2. Molecules 24:4534. https://doi.org/10.3390/molecules24244534

Campisi S, Schiavoni M, Chan-Thaw CE, Villa A (2016) Untangling the role of the capping agent in nanocatalysis: recent advances and perspectives. Catalysts 6:185. https://doi.org/10.3390/catal6120185

Cao H (2017) Synthesis, characterization, and applications of zero-dimensional (0D) nanostructures. https://doi.org/10.1002/9783527698158.ch2. Accessed 20 May 2019

Cao D, Gong S, Shu X, Zhu D, Liang S (2019) Preparation of ZnONPs with high dispersibility based on oriented attachment process. Nanoscale Res Lett 14:210. https://doi.org/10.1186/s11671-019-3038-3

Chakraborty A, Saha BB, Ng KC, Koyama S, Srinivasan K (2009) Heoretical insight of physical adsorption for a single-component adsorbent + adsorbate system: I. Thermodynamic property surfaces. Langmuir 25(4):2204–2211. https://doi.org/10.1021/la803289p

Chandramohan K, Valli R, Mageswari B (2017) Synthesis and characterization of zinc nanopartical from luffa acutangula. Int J Sci Res 6(11):339–340

Chitra K, Annadurai G (2014) antibacterial activity of ph-dependent biosynthesized silver nanoparticles against clinical pathogen. Biomed Res Int. https://doi.org/10.1155/2014/725165

Chitha MJ, Sathya M, Pushpanathan K (2015) Effect of pH on crystal size and photoluminescence property of ZnONPs prepared by chemical precipitation method. Acta Metall Sin (Engl Lett) 28(3):394–404. https://doi.org/10.1007/s40195-015-0218-8

Christmann K (2010) Adsorption. Lecture series 2010/2011: "Modern Methods in Heterogeneous Catalysis Research Institut für Chemie und Biochemie, Freie Universität, Berlin. http://www.fhierlin.mpg.de/acnew/department/pages/teaching/pages/teaching_wintersemester_2010_2011/klaus_christmann_adsorption_101105.pdf. Accessed 23 June 2018

Dalod ARM, Grendal OG, Skjærvø SL, Inzani K, Selbach SM, Henriksen L, Beek WV, Grande T, Einarsrud M (2017) Controlling oriented attachment and in situ functionalization of TiO2 nanoparticles during hydrothermal synthesis with APTES. J Phys Chem 121(21):11897–11906. https://doi.org/10.1021/acs.jpcc.7b02604

Dange SS, Dange SN, More PS (2015) Effect of pH on morphology of Cu added ZnO nanostructures by precipitation method. Int J Innov Res Sci Eng Technol 4(9):8637–8642. https://doi.org/10.15680/IJIRSET.2015.0409131

Degen A, Kosec M (2000) Effect of pH and impurities on the surface charge of zinc oxide in aqueous solution. J Eur Ceram Soc 20:667–673. https://doi.org/10.1016/S0955-2219(99)00203-4

Duan P, Yan C, Zhou W, Ren D (2016) Development of fly ash and iron ore tailing based porous geopolymer for removal of Cu(II) from wastewater. Ceram Int 42:13507–13518

Eadi SB, Kim S, Jeong SO (2017) Effect of surfactant on growth of ZnO nanodumbbells and their characterization. J Chem. https://doi.org/10.1155/2017/1728345

Engwa GA, Ferdinand PU, Nwalo FN, Unachukwu MN (2016) Mechanism and health effects of heavy metal toxicity in humans, pp 1–23. https://www.intechopen.com/books/poisoning-in-the-modern-world-new-tricks-for-an-old-dog-/mechanism-and-health-effects-of-heavy-metal-toxicity-in-humans

Erhard N, Holleitner A (2015) 13-Semiconductor nanowires studied by photocurrent spectroscopy semiconductor nanowires materials, synthesis, characterization and applications. Series in electronic and optical materials, pp 365–391. https://www.elsevier.com/books/semiconductor-nanowires/arbiol/978-1-78242-253-2

Etcheverry LP, Flores WH, Silva DL, Moreira EC (2017) Annealing effects on the structural and optical properties of ZnO nanostructures. Mater Res 21(2):1–7. https://doi.org/10.1590/1980-5373-mr-2017-0936

Ezhilarasi AA, Vijaya JJ, Kennedy JL, Vasanth M (2016) Green synthesis of Mg doped zinc oxide nanoparticles using aloe vera plant extract and its characterization. J Chem Pharma Sci 9(3):1450–1453

Fakhari S, Jamzad M, Fard HF (2019) Green synthesis of zinc oxide nanoparticles: a comparison. Green Chem Lett Rev 12(1):19–24. https://doi.org/10.1080/17518253.2018.1547925

Geetha A, Sakthivel R, Mallika J, Kannusamy R, Rajendran R (2016) Green synthesis of antibacterial zinc oxide nanoparticles using biopolymer *Azadirachta indica* gum. Orient J Chem 32(2):955–963. https://doi.org/10.13005/ojc/320222

Getie S, Belay A, Chandra Reddy AR, Belay Z (2017) Synthesis and characterizations of zinc oxide nanoparticles for antibacterial applications. J Nanomed Nanotechnol. https://doi.org/10.4172/2157-7439.S8-004

Ghannam H, Chahboun A, Turmine M (2019) Wettability of zinc oxide nanorod surfaces. R Soc Chem Adv 9:38289–38297. https://doi.org/10.4172/2157-7439.S8-004

Ghassan AA, Mijan N, Taufiq-Yap YH (2019) Nanomaterials: an overview of nanorods synthesis and optimization. https://doi.org/10.5772/intechopen.84550. Accessed 20 May 2020

Girish CR, Murty VR (2017) Mass transfer studies on adsorption of phenol from wastewater using lantana camara, forest waste. Int J Chem Eng. https://doi.org/10.1155/2016/5809505

Gopal VRV, Kamila S (2017) Effect of temperature on the morphology of ZnONPs: a comparative study. Appl Nanosci 7:75–82. https://doi.org/10.1007/s13204-017-0553-3

Goryacheva IY (2016) Chapter 4—labels for optical immunotests. In: Comprehensive analytical chemistry, vol 72, pp 79–131. https://www.sciencedirect.com/handbook/comprehensive-analytical-chemistry/vol/72/suppl/C. Accessed 20 May 2019

Gulati S, Sachdeva M, Bhasin KK (2016) Capping agents in nanoparticle synthesis: Surfactant and solvent system. In: AIP conference proceedings. https://doi.org/10.1063/1.5032549. Accessed June 2020

Gunatilake SK (2015) Methods of removing heavy metals from industrial wastewater. J Multidiscip Eng Sci Stud: JMESS 1(1):12–18

Gupta VK, Suhas A, Nayak S, Chaudhary AM, Tyagi I (2014) Removal of Ni (II) ions from water using scrap tire. J Mol Liquids 190:215–222. https://doi.org/10.1016/j.molliq.2013.11.008

Gusatti M, Barroso GS, Campos CEM, Souza DAR, Rosário JA, Lima RB, Silva LA, Riella HG, Kuhnen NC (2011) Effect of different precursors in the chemical synthesis of ZnO nanocrystals. Effect of different precursors in the chemical synthesis of ZnO nanocrystals. Mater Res. https://doi.org/10.1590/S1516-14392011005000035

Hajiashafi S, Motakef-Kazemi N (2018) Green synthesis of zinc oxide nanoparticles using parsley extract. Nanomed Res J 3(1):44–50. https://doi.org/10.22034/nmrj.2018.01.007

Harun K, Mansor N, Ahmad ZA, Mohamad AZ (2016) Electronic properties of ZnONPs synthesized by sol–gel method: a LDA+ U calculation and experimental study. Procedia Chem 19:125–132. https://doi.org/10.1016/j.proche.2016.03.125

Hasan M, Ullah I, Zulfiqar H, Naeem K, Iqbal A, Gul H, Ashfaq M, Mahmood N (2018) Biological entities as chemical reactors for synthesis of nanomaterials: progress, challenges and future perspective. Mater Today Chem 8:13–28. https://doi.org/10.1016/j.mtchem.2018.02.003

Hasanpoor M, Aliofkhazraei M, Delavari H (2015) Microwave-assisted synthesis of zinc oxide nanoparticles. Procedia Mater Sci 11:320–325. https://doi.org/10.1016/j.mspro.2015.11.101

Hedayati K (2016) Fabrication and optical characterization of zinc oxide nanoparticles prepared via a simple sol–gel method. J Nanostruct 5:395–401. https://doi.org/10.7508/JNS.2015.04.010

Herrera-Rivera R, Olvera R, Maldonado A (2017) Synthesis of ZnO nanopowders by the homogeneous precipitation method: use of taguchi's method for analyzing the effect of different variables. J Nanomater 1:1. https://doi.org/10.1155/2017/4595384

Hu H, Huang X, Deng C, Chen X, Qian Y (2007) Hydrothermal synthesis of ZnO nanowires and nanobelts on a large scale. Mater Chem Phys 106:58–62. https://doi.org/10.1016/j.matchemphys.2007.05.016

Iftekhar S, Ramasamy DL, Srivastava V, Asif MB, Sillanpa M (2018) Understanding the factors affecting the adsorption of Lanthanum using different adsorbents: a critical review. Chemosphere 204:413–430. https://doi.org/10.1016/j.chemosphere.2018.04.053

Ihsanullah AFA, Al-Khaldi FA, Abusharkh B, Khaled M, Atieh MA et al (2015) Adsorptive removal of cadmium (II) ions from liquid phase using acid modified carbon-based adsorbents. J Mol Liquids 204:255–263. https://doi.org/10.1016/j.molliq.2015.01.033

Ikono R, Akwalia PR, Bambang W, Sukarto A, Rochman NT (2012) Effect of PH variation on particle size and purity of nano zinc oxide synthesized by sol–gel method. Int J Eng Technol: IJET IJENS 2(6):1–9

Indramahalakshmi G (2017) Characterization and antibacterial activity of zinc oxide nanoparticles synthesized using *Opuntia ficus indica* fruit aqueous extract. Asian J Phys Chem Sci 3(2):1–7. https://doi.org/10.9734/AJOPACS/2017/35917

Jadhav NA, Singh PK, Rhee HW, Bhattacharya B (2014) Effect of variation of average pore size and specific surface area of ZnO electrode (WE) on efficiency of dye-sensitized solar cells. Nanoscale Res Lett 9:575

Jamal A, Awad R, Yusef H (2019) Evaluation of antimicrobial activity of ZnONPs against foodborne pathogens. Int J Curr Microbiol Appl Sci 8(11):2000–2025. https://doi.org/10.20546/ijcmas

Jin XYuC, Li Y, Qi Y, Yang L, Zhao G, Hu H (2011) Preparation of novel nano-adsorbent based on organic–inorganic hybrid and their adsorption for heavy metals and organic pollutants presented in water environment. J Hazard Mater 186:1672–1680

Jin X, Götz M, Wille S, Mishra YK, Adelung R, Zollfrank C (2013) A novel concept for self-reporting materials: stress sensitive photoluminescence in ZnO tetrapod filled elastomers. Adv Mater 25(9):1342. https://doi.org/10.1002/adma.201203849

Kahaman O, Binzet R, Turunc E, Dogen A, Arslan H (2018) Synthesis, characterization, antimicrobial and electrochemical activities of zinc oxide nanoparticles obtained from *Sarcopoterium spinosum* (L) spach leaf extract. Mater Res Express 5(11):1–10. https://doi.org/10.1088/2053-1591/aad953

Kamath S, Gopal V, Ramanjaneyalu V, Kamila S (2018) Application of ZnO nano rods for the batch adsorption of Cr (VI): a study of kinetics and isotherms. Am J Appl Sci 16(3):1–12. https://doi.org/10.3844/ajassp.2019.101.112

Kayani ZN, Saleemi F, Batool I (2015) Effect of calcination temperature on the properties of ZnONPs. Appl Phys A. https://doi.org/10.1007/s00339-015-9019-1

Khan M, Hameedullah M, Ansari A, Ahmad E, Khan RL, Alam M, Khan W, Husain FM, Ahmad I (2014) Flower-shaped ZnONPs synthesized by a novel approach at near-room temperatures with antibacterial and antifungal properties. Int J Nanomed 9(1):853–864. https://doi.org/10.2147/IJN.S47351

Koao LF, Dejene FB, Swart HC (2015) Effect of pH on the properties of ZnO nanostructures prepared by chemical bath deposition method. In: Proceedings of SAIP2015. https://www.researchgate.net/publication/306000264_Effect_of_pH_on_the_properties_of_ZnO_nanostructures_prepared_by_chemical_bath_deposition_method. Accessed 12 Feb 2020

Kołodziejczak-Radzimska A, Markiewicz E, Jesionowski T (2012) Structural characterisation of ZnO particles obtained by the emulsion precipitation method. J Nanomater. https://doi.org/10.1155/2012/656353

Koutu V, Shastri L, Malik MM (2016) Effect of NaOH concentration on optical properties of zinc oxide nanoparticles. Mater Sci Pol 34(4):819–827. https://doi.org/10.1515/msp-2016-0119

Kumar SS, Venkateswarlu P, Rao VR, Rao GN (2013) Synthesis, characterization and optical properties of zinc oxide nanoparticles. Int Nano Lett 3:1–6. https://doi.org/10.1186/2228-5326-3-30

Kumari M, Misha A, Pandey S, Singh SP, Chaudhy V, Mudiam MKR, Shukla S, Kakkar P, Nautiyal CS (2016) Physico-chemical condition optimization during biosynthesis led to development of improved and catalytically efficient gold nano particles. Sci Rep 6:27575

Kvitek L, Prucek K, Panacek A, Soukupova J (2016) Physicochemical aspects of metal nanoparticle preparation, pp 1–34. https://doi.org/10.5772/intechopen.89954. Accessed 12 April 2020

Kyoung-Ku K, Byungjin L, Chang-Soo L (2019) Recent progress in the synthesis of inorganic particulate materials using microfluidics. J Taiwan Inst Chem Engi 98:2–19. https://doi.org/10.1016/j.jtice.2018.08.027

Kyzas GZ, Kostoglou M (2014) Green adsorbents for wastewaters: a critical review. Materials (Basel) 7(1):333–364. https://doi.org/10.3390/ma7010333

Ladu JLC, Athiba AL, Lako STV, Alfred ML (2018) Investigation on the impact of water pollution on human health in Juba County, Republic of South Sudan. J Environ Pollut Hum Health 6(3):89–95. https://doi.org/10.12691/jephh-6-3-2

Lata S, Singh PK, Samadder SR (2019) Regeneration of adsorbents and recovery of heavy metals: a review. Int J Environ Sci Technol 12:1461–1478. https://doi.org/10.1007/s13762-014-0714-9

Layek A, Misha G, Sharma A, Spasova M, Dhar M, Chowdhury A, Bandyopadhyaya R (2012) A generalized three-stage mechanism of ZnO nanoparticle formation in homogeneous liquid medium. J Phys Chem 116:24757–24769. https://doi.org/10.1021/jp211613b

Leonardi SG (2017) Two-dimensional zinc oxide nanostructures for gas sensor applications. Chemosensors 5(17):1–28. https://doi.org/10.3390/chemosensors5020017

Liu H, Zhang H, Wang J, Wei J (2020) Effect of temperature on the size of biosynthesized silver nanoparticle: deep insight into microscopic kinetics analysis. Arab J Chem 13(1):1011–1019

Ma J, Zuo-Jiang S, He Y, Sun Q, Wang Y, Liu W, Sun S, Chen K (2016) A facile, versatile approach to hydroxyl-anchored metal oxides with high Cr(VI) adsorption performance in water treatment. R Soc Open Sci 3(11):160524. https://doi.org/10.1098/rsos.160524

Maduabuchi MN (2018) Agricultural waste materials as a potential adsorbent for removal of heavy metals in wastewater. J Waste Manag Xenobiotics 1(1):1–4. https://doi.org/10.23880/oajwx-16000104

Mahdavi S, Jalali M, Afkhami A (2012) Removal of heavy metals from aqueous solutions using Fe_3O_4, ZnO, and CuO nanoparticles. J Nanopart Res 14:846. https://doi.org/10.1007/s11051-012-0846-0

Mahmoodian H, Moradi O, Shariatzadeha B, Saleh TA, Tyagi I, Maity A, Asif M, Gupta KV (2015) Enhanced removal of methyl orange from aqueous solutions by poly HEMA-chitosan-MWCNT nano-composite. J Mol Liquids 202:189–198. https://doi.org/10.1016/j.molliq.2014.10.040

Mahmoud MA (2015) Kinetics and thermodynamics of aluminum oxidenanopowder as adsorbent for Fe (III) from aqueoussolution. Beni-Suef Univ J Basic Appl Sci 4(2015):142–149. https://doi.org/10.1016/j.molliq.2014.10.040

Mallika NA, Reddy AR, Reddy KV (2015) Annealing effects on the structural and optical properties of ZnONPs with PVA and CA as chelating agents. J Adv Ceram 4(2):123–129. https://doi.org/10.1007/s40145-015-0142-4

Manzoor U, Zaha FT, Rafique S, Moin MT, Mujahid M (2015) Effect of synthesis temperature, nucleation time, and postsynthesis heat treatment of ZnONPs and its sensing properties. J Nanomater. https://doi.org/10.1155/2015/189058

Marcus C, Paul N, Warburton A (2007) ZnO tetrapod nanocrystals. Mater Today 10(5):50–54. https://doi.org/10.1016/S1369-7021(07)70079-2

Mathew BB, Jaishankar M, Biju VG, Beeregowda KN (2016) Role of bioadsorbents in reducing toxic metals. J Toxicol 1:1. https://doi.org/10.1155/2016/4369604

Mayekar J, Dhar V, Radha S (2014) Role of salt precursor in the synthesis of zinc oxide nanoparticles. Int J Res Eng Technol 3(3):43–45. https://doi.org/10.15623/ijret.2014.0303008

Meenakshi G, Sivasamy A (2017) Synthesis and characterization of zinc oxide nanorods and its photocatalytic activities towards degradation of 2,4-D. Ecotoxicol Environ Saf 135:243–325

Moazzen MA, Borghei SM, Taleshi F (2013) Change in the morphology of ZnONPs upon changing the reactant concentration. Appl Nanosci 3:295–302. https://doi.org/10.1007/s13204-012-0147-z

Modi G (2015) Zinc oxide tetrapod: a morphology with multifunctional applications advances in natural sciences. Nanosci Nanotechnol 6:1–8. https://doi.org/10.1088/2043-6262/6/3/033002

Moghaddam AB, Moniri M, Azizi S, Rahim RA, Ariff AB, Saad WZ, Namvar F, Navaderi M, Mohamad R (2017) Biosynthesis of ZnONPs by a new *Pichia kudriavzevii* yeast strain and evaluation of their antimicrobial and antioxidant activities. Molecules 22(6):872

Mohammadi FM, Ghasemi N (2018) Influence of temperature and concentration on biosynthesis and characterization of zinc oxide nanoparticles using cherry extract. J Nanostruct Chem 8:93–102. https://doi.org/10.1007/s40097-018-0257-6

Monisha J, Tenzin T, Naresh A, Blessy BM, Krishnamurthy NB (2014) Toxicity, mechanism and health effects of some heavy metals. Interdiscip Toxicol 7(2):60–72. https://doi.org/10.2478/intox-2014-0009

Mornani EG, Mosayebian P, Dorranian D, Behzad K (2016) Effect of calcination temperature on the size and optical properties of synthesized ZnONPs. J Ovonic Res 12(2):75–80

Mrad M, Chouchene B, Chaabane TB (2018) Effects of zinc precursor, basicity and temperature on the aqueous synthesis of ZnO nanocrystals. S Afr J Chem 71:103–110. https://doi.org/10.17159/0379-4350/2018/v71a13

Nalwa K, Thakur A, Sharma N (2017) Synthesis of ZnONPs and its application in adsorption. Adv Mater Proc 2(11):697–703. https://doi.org/10.5185/amp/2017/696

Nasrollahzadeh M, Issaabadi Z, Sajjadi M, Sajadi M, Atarod M (2019) Chapter 2-types of nanostructure. Interface Sci Technol 28:29–80

Nejati K, Rezvani Z, Pakizevand R (2016) Synthesis of ZnONPs and investigation of the ionic template effect on their size and shape. Int Nano Lett 1(2):75–81

Ogbomida ET, Nakayama S, Bortey-Sam N, Oroszlany B, Tongo I, Enuneku AA, Ogbeide O, Ainerua MO, Fasipe IP, Ezemonye LI, Mizukawa H, Ikenaka Y, Ishizuka IM (2018) Accumulation patterns and risk assessment of metals and metalloid in muscle and official of free-range chickens, cattle and goat in Benin City, Nigeria. Ecotoxicol Environ Saf 151:98–108. https://doi.org/10.1016/j.ecoenv.2017.12.069

Osman DAM, Mustafa MA (2015) Synthesis and characterization of zinc oxide nanoparticles using zinc acetate dihydrate and sodium hydroxide. J Nanosci Nanoeng 1(4):248–251

Ouyang TD, Zhuo YZ, Hu L, Zeng Q, Hu Y, He Z (2019) Research on the adsorption behavior of heavy metal ions by porous material prepared with silicate. Minerals 9(291):1–16. https://doi.org/10.3390/min9050291

Özgür Ü, Alivov YI, Liu C, Teke A, Reshchikov M, Doğan S, Avrutin VC, Cho SJ, Morkoç AH (2005) A comprehensive review of ZnO materials and devices. J Appl Phys 98(4):041301. https://doi.org/10.1063/1.1992666

Parihar V, Raja M, Paulose R (2018) A brief review of structural, electrical and electrochemical properties of zinc oxide nanoparticles. Rev Adv Mater Sci 53:119–130. https://doi.org/10.1515/rams-2018-0009

Parra MR, Haque FZ (2014) Aqueous chemical route synthesis and the effect of calcination temperature on the structural and optical properties of ZnONPs. J Mater Technol 3(4):363–369. https://doi.org/10.1016/j.jmrt.2014.07.001

Pelicano CM, Magdaluyo E, Ishizumi A (2016) Temperature dependence of structural and optical properties of ZnONPs formed by simple precipitation method. In: MATEC Web of conferences, published by EDP sciences, vol 43, pp 1–4

Peng S, Wu G, Song W, Wang Q (2013) Application of flower-like ZnO nanorods gas sensor detecting SF_6 decomposition products. J Nanomater. https://doi.org/10.1155/2013/135147

Peng H, Sun X, Weng W, Fang X (2017) 4—electronic polymer composite polymer materials for energy and electronic applications, pp 107–149. https://doi.org/10.1016/C2015-0-01541-6. Accessed 20 May 2020

Perillo PM, Atia MN, Rodríguez DF (2018) Studies on the growth control of ZnO nanostructures synthesized by the chemical method. Revista Matér 23(2):1–7. https://doi.org/10.1590/S1517-707620180002.0467

Perveena R, Shujaat S, Qureshi Z, Nawaz S, Khand MI, Iqbal M (2020) Green versus sol–gel synthesis of ZnONPs and antimicrobial activity evaluation against panel of pathogens. J Mater Res Technol 9:7817–7827. https://doi.org/10.1016/j.jmrt.2020.05.004

Phan CM, Nguyen HM (2017) Role of capping agent in wet synthesis of nanoparticles. Phys Chem A 121(17):3213–3219. https://doi.org/10.1021/acs.jpca.7b02186

Polte J, Ahner TT, Delissen F, Sokolov S, Emmerling F, Thuenemann AF, Kraehnert R (2010) Mechanism of gold nanoparticle formation in the classical citrate synthesis method derived from coupled in situ XANES and SAXS evaluation. J Am Chem Soc 132:1296–1301. https://doi.org/10.1021/ja906506j

Purwaningsih SY, Pratapa S, Darminto T (2016) Synthesis of nanosized ZnO particles by co-precipitation method with variation of heating time. In: AIP conference proceedings, vol 1710, no 1. https://doi.org/10.1063/1.4941506

Pushpanathan K, Sathya M, Chitha MJ, Gowthami S, Santhi R (2012a) Influence of reaction temperature on crystal structure and band gap of ZnONPs. Mater Manuf Process 27(12):1–10. https://doi.org/10.1080/10426914.2012.700163

Pushpanathan K, Sathya S, Chithra SJ, Gowthami S, Santhi R (2012b) Influence of reaction temperature on crystal structure and band gap of ZnONPs. Mater Manuf Process 27(12):1334–1342. https://doi.org/10.1080/10426914.2012.700163

Rafaie HA, Samat NA, MdNora R (2014) Effect of pH on the growth of zinc oxide nanorods using *Citrus aurantifolia* extracts. Mater Lett 137:297–299. https://doi.org/10.1016/j.matlet.2014.09.033

Raliya R, Tarafdar JC (2013) Biosynthesis and characterization of zinc, magnesium and titanium nanoparticles: an eco-friendly approach. Int Nano Lett 4:1–93. https://doi.org/10.1007/s40089-014-0093-8

Ravangave LS, Shaikh RS (2017) Influence of pH on structure, morphology and UV–visible spectra of ZnO nanorod. Int J Eng Sci Invent 6(11):76–79

Ray PZ, Shipley HJ (2015) Inorganic nano-adsorbents for the removal of heavy metals and arsenic: a review. RSC Adv 5(38):29885–29907. https://doi.org/10.1039/C5RA02714D

Rezende CP, Silva JB, Mohallem NDS (2009) Influence of drying on the characteristics of zinc oxide nanoparticles. Braz J Phys 39(1a):248–251. https://doi.org/10.1590/s0103-97332009000200022

Ribut SH, Abdullah CA, Mustafa M, Yusoff MZM, Azman SNA (2018) Influence of pH variations on zinc oxide nanoparticles and their antibacterial activity. Mater Res Express 6(2):1–9

Ruszkiewicz JA, Pinkas A, Ferrer B, Peres TV, Tsatsakis A, Aschner M (2017) Neurotoxic effect of active ingredients in sunscreen products, a contemporary review. Toxicol Rep 4:245–259. https://doi.org/10.1016/j.toxrep.2017.05.006

Ruys A (2019) 15-Refractory and other specialist industrial applications of alumina. Biomed Clin Appl. https://doi.org/10.1016/C2017-0-01189-8

Salahuddin NA, El-Kemary M, Ibrahim EM (2015) Synthesis and characterization of ZnONPs via precipitation method: effect of annealing temperature on particle size. Nanosci Nanotechnol 5(4):82–88. https://doi.org/10.5923/jnn2015050402

Salmani MH, Zarei S, Ehrampoush MH, Danaie S (2013) Evaluations of pH and high ionic strength solution effect in cadmium removal by zinc oxide nanoparticles. J Appl Sci Environ Manag 17(4):583–593. https://doi.org/10.4314/jasem.v17i4.17

Samei J, Shokuhfar A, Kandjani AE, Vaezi MR (2008) Effect of synthesis temperature on the morphology of ZnO nanoparticles obtained via a novel chemical route. Defect Diffus Forum 273–276:192–197. https://doi.org/10.4028/www.scientific.net/ddf.273-276.192

Sandhyarani N (2019) Surface modification methods for electrochemical biosensors. Electrochem Biosens. https://doi.org/10.1016/b978-0-12-816491-4.00003-6

Savi BM, Rodrigues L, Bernardin AM (2018) Synthesis of ZnONPs by solgel. Process Castellón (Spain) 1(8):1–8

Saxena J, Sharma PK, Sharma MM, Singh A, Fu Y (2016) Process optimization for green synthesis of silver nanoparticles by *Sclerotinia sclerotiorum* MTCC 8785 and evaluation of its antibacterial properties. SpringerPlus 5(861):1–10. https://doi.org/10.1186/s40064-016-2558-x

Senol SD, Yalcin B, Ozugurlu E, Arda EL (2020) Structure, microstructure, optical and photocatalytic properties of Mn doped ZnONPs. Mater Res Express 1(1):1–18. https://doi.org/10.1088/2053-1591/ab5eea

Shaikh RS, Ravangave LS (2015) Effect of reaction time on some characterization of ZnONPs. Int Res J Sci Eng Spec Issue A2:187–191

Shaikh RS, Rakh RR, Ravangave LS (2016) Sol–gel precipitation synthesis of ZnONPs, their morphological changes after calcinations and antibacterial properties. Int Res J Sci Eng 4(1):31–35

Sharma SA, Kumar SK, Rajesh N (2017) A perspective on diverse adsorbent materials to recover precious palladium and the way forward. R Soc Chem Adv 7:2133–52142. https://doi.org/10.1039/C7RA10153H

Shende P, Kasture P, Gaud RS (2018) Nanoflowers: the future trend of nanotechnology for multi-applications, artificial cells. Nanomed Biotechnol 46:413–422. https://doi.org/10.1080/21691401.2018.1428812

Sierra MJ, Herrera AP, Ojeda KA (2018) Synthesis of zinc oxide nanoparticles from mango and soursop leaf extracts. Contemp Eng Sci 11(8):395–403. https://doi.org/10.12988/ces.2018.82281

Singh RP, Hudiara IS, Rana SB (2016) Effect of calcination temperature on the structural, optical and magnetic properties of pure and Fe-doped ZnONPs. Mater Sci Pol 34(4):451–459. https://doi.org/10.1515/msp-2016-0059

Singh J, Yadav P, Pal AK, Mishra V (2018) Water pollutants: origin and status. Sens Water Pollut Monit Role Mater. https://doi.org/10.1007/978-981-15-0671-0_2

Siswanto RNT, Akwalia PR (2017) Fabrication and characterization of zinc oxide (ZnO) nanoparticle by sol–gel method. . IOP Conf Ser J Phys Conf Ser 853:1–5. https://doi.org/10.1088/1742-6596/853/1/012041

Smolkova IS, Kazantseva NE, Babayan V, Pizurova NJV, Saha P (2017) The role of diffusion-controlled growth in the formation of uniform iron oxide nanoparticles with a link to magnetic hyperthermia. Cryst Growth Des 17(5):2323–2332

Subramanian KR (2018) The crisis of consumption of natural resources. Int J Recent Innov Acad Res 2(4):8–19

Swaroop K, Somashekarappa HM (2014) Effect of pH values on surface morphology and particle size variation in ZnONPs synthesised by co-precipitation method. Res J Recent Sci 4:197–201

Tan ST, Umar AA, Salleh MM (2015) (001)-Faceted hexagonal ZnO nanoplate thin film synthesis and the heterogeneous catalytic reduction of 4-nitrophenol characterization. J Alloy Compd 650:299–304. https://doi.org/10.1016/j.jallcom.2015.06.280

Thanh NK, Maclean N, Mahiddine S (2014) Mechanisms of nucleation and growth of nanoparticles in solution. Chem Rev 14(15):7610–7630

Tourné-Péteilh C, Robin B, Lions M, Martinez J, Mehdi A, Subra G, Devoisselle JM (2018) Combining sol–gel and microfluidics processes for the synthesis of protein-containing hybrid microgels. Chem Commun 55:13112–13115

Tseng Y, Chuang M, Chen Y, Wu C (2012) Synthesis of 1D, 2D, and 3D ZnO polycrystalline nanostructures using the sol–gel method. J Nanotechnol. https://doi.org/10.1155/2012/712850

Ul-Haq AN, Nadhman A, Ullah I, Mustafa G, Yasinzai M, Khan I (2017) Synthesis approaches of zinc oxide nanoparticles: the dilemma of ecotoxicity. J Nanomater 42:1–14

Umar H, Kavaz D, Rizaner N (2019) Biosynthesis of zinc oxide nanoparticles using *Albizia lebbeck* stem bark, and evaluation of its antimicrobial, antioxidant, and cytotoxic activities on human breast cancer cell lines. Int J Nanomed 14:87–100. https://doi.org/10.2147/IJN.S186888

UNEP-Global (2009) Marine litter: a global challenge. UNEP, Athens. ISBN 9789280730296. https://www.google.com/search?q=UNEP-Global.+Marine+Litter%3A+A+Global+Challenge%3B+UNEP%3A+Athens%2C+Greece%2C+2009%3B+ISBN+9789280730296&oq=UNEP-Global.+Marine+Litter%3A+A+Global+Challenge%3B+UNEP%3A+Athens%2C+Greece%2C+2009%3B+ISBN+9789280730296&aqs=chrome..69i57.545j0j7&sourceid=chrome&ie=UTF-8. Accessed 15 April, 2020. Accessed May 2020

Verma N, Bhatia S, Bedi RK (2017) Effect of annealing temperature on ZnONPs and its applications for photocatalytic degradation of DR-31 dye. Int J Pure Appl Phys 13(1):118–122

Wang L, Zhang X (2005) Synthesis of well-aligned ZnO nanowires by simple physical vapor deposition on cc-oriented ZnO thin films without catalysts or additives. Appl Phys Lett 86(2):024108. https://doi.org/10.1063/1.1851607

Wang Y, Cui Z (2009) Synthesis and photoluminescence of well aligned ZnO nanotube arrays by a simple chemical solution method. J Phys Conf Ser 152:1–5. https://doi.org/10.1088/1742-6596/152/1/012021

Waqar S, Wang L, John S (2015) Piezoelectric energy harvesting from intelligent textiles. Electron Text. https://doi.org/10.1016/b978-0-08-100201-8.00010-2

Westen TV, Groot RD (2018) Effect of temperature cycling on ostwald ripening. Cryst Growth Des 8(9):4952–4962. https://doi.org/10.1021/acs.cgd.8b00267

Wołowiec M, Komorowska-Kaufman M, Pruss A, Rzepa A, Bajda T (2019) Removal of heavy metals and metalloids from water using drinking water treatment residuals as adsorbents: a review. Minerals 9(8):1–17. https://doi.org/10.3390/min9080487

Xie J, Lin Y, Li C, Wu D, Kong H (2015) Removal and recovery of phosphate from water by activated aluminum oxide and

lanthanum oxide. Powder Technol 269:351–357. https://doi.org/10.1016/j.powtec.2014.09.024
Yu H, Dong Y (2016) Investigation of ZnO nanostructures synthesized from different zinc salts. ChemXpress 9(1):091–097
Yuvaraja G, Prasad C, Vijaya Y, Subbaiah MV (2018) Application of ZnO nanorods as an adsorbent material for the removal of As(III) from aqueous solution: kinetics, isotherms and thermodynamic studies. Int J Ind Chem 9:17–25. https://doi.org/10.1007/s40090-018-0136-5
Zhang J, Huang F, Lin Z (2010) Progress of nanocrystalline growth kinetics based on oriented attachment. Nanoscale 2:18–34. https://doi.org/10.1039/b9nr00047j.Epub2009Oct5
Zhang C, Xie B, Zou Y, Zhu D, Lei L, Zhao D, Nie H (2018) Zero-dimensional, one-dimensional, two-dimensional and three-dimensional biomaterials for cell fate regulation. Adv Drug Deliv Rev 132:33–56. https://doi.org/10.1016/j.addr.2018.06.020
Ziółkowska M, Milewska-Duda J, Duda JT (2016) Effect of adsorbate properties on adsorption mechanisms: computational study. Adsorption 22:589–597. https://doi.org/10.1007/s10450-015-9736-y